

No Evidence of Winter Warming in Eurasia Following Large, Low-Latitude Volcanic Eruptions during the Last Millennium

ERNESTO TEJEDOR,^a LORENZO M. POLVANI,^{b,c} NATHAN J. STEIGER,^{c,d}
MATHIAS VUILLE,^e AND JASON E. SMERDON^f

^a *Department of Geology, National Museum of Natural Sciences-Spanish National Research Council (MNCN-CSIC), Madrid, Spain*

^b *Department of Applied Physics and Applied Mathematics, Columbia University, New York, New York*

^c *Lamont-Doherty Earth Observatory, Columbia University, Palisades, New York*

^d *Institute of Earth Sciences, Hebrew University of Jerusalem, Jerusalem, Israel*

^e *Department of Atmospheric and Environmental Sciences, University at Albany, State University of New York, Albany, New York*

^f *Columbia Climate School, Columbia University, New York, New York*

(Manuscript received 16 October 2023, in final form 7 June 2024, accepted 24 June 2024)

ABSTRACT: We critically reexamine the question of whether volcanic eruptions cause surface warming over Eurasia in winter, in the light of recent modeling studies that have suggested internal variability may overwhelm any forced volcanic response, even for the very largest eruptions during the Common Era. Focusing on the last millennium, we combine model output, instrumental observations, tree-ring records, and ice cores to build a new temperature reconstruction that specifically targets the boreal winter season. We focus on 20 eruptions over the last millennium with volcanic stratospheric sulfur injections (VSSIs) larger than the 1991 Pinatubo eruption. We find that only 7 of these 20 large events are followed by warm surface temperature anomalies over Eurasia in the first posteruption winter. Examining the 13 events that show cold posteruption anomalies, we find no correlation between the amplitude of winter cooling and VSSI mass. We also find no evidence that the North Atlantic Oscillation is correlated with VSSI in winter, a key element of the proposed mechanism through which large, low-latitude eruptions might cause winter warming over Eurasia. Furthermore, by inspecting individual eruptions rather than combining events into a superposed epoch analysis, we are able to reconcile our findings with those of previous studies. Analysis of two additional paleoclimatic datasets corroborates the lack of posteruption Eurasian winter warming. Our findings, covering the entire last millennium, confirm the findings of most recent modeling studies and offer important new evidence that large, low-latitude eruptions are not, in general, followed by significant surface wintertime warming over Eurasia.


KEYWORDS: Volcanoes; Stratosphere-troposphere coupling; Climate records; Tree rings; Climate variability; North Atlantic Oscillation

1. Introduction

The idea that volcanic eruptions cause surface warming in the boreal winter over the Eurasian continent originated from several noteworthy papers that appeared in the years following the Pinatubo eruption in June 1991. On the basis of a dozen eruptions over the last two centuries, these papers proffered observational (e.g., Robock and Mao 1992, 1995) and modeling (e.g., Graft et al. 1993; Kirchner et al. 1999) evidence showing that posteruption surface warming over the northern continents could be a consequence of volcanic aerosols. While surprising at first, because one naïvely expects cooling from reduced insolation in the presence of volcanic aerosols, these early papers proved greatly influential, in large part because their claims were based on a physically plausible mechanism, which we refer to here as “the stratospheric pathway” (e.g., Graft et al. 1993; Kodera 1994).

In a nutshell, the stratospheric pathway consists of the following sequence of events: 1) volcanic aerosols from a low-latitude eruption—being longwave absorbers—produce significant warming in the tropical lower stratosphere; 2) through thermal wind balance, the tropical stratospheric warming results in a strengthening of the winter stratospheric polar vortex; and 3) this strengthening causes a positive phase of the North Atlantic Oscillation (NAO), which in turn induces downstream warm surface temperature anomalies over Eurasia. It is important to emphasize two sine qua non conditions for this mechanism to be operative. First, the eruption needs to occur at low latitudes, where the upwelling stratospheric circulation allows the aerosols to remain in the stratosphere for months following the eruption. Second, the surface effect it induces would only exist in the winter months, as the stratospheric polar vortex only exists between November and March.

While the belief that low-latitude volcanic eruptions can cause boreal winter warming, via the stratospheric pathway, quickly became widely accepted, subsequent observational and modeling studies reported surprising results. For instance, Fischer et al. (2007)—the latest and most comprehensive paleoclimatic study—analyzed 15 low-latitude eruptions after the year 1500 using a temperature reconstruction over Europe

 Denotes content that is immediately available upon publication as open access.

Corresponding author: Lorenzo Polvani, Imp@columbia.edu

DOI: 10.1175/JCLI-D-23-0625.1

© 2024 American Meteorological Society. This published article is licensed under the terms of the default AMS reuse license. For information regarding reuse of this content and general copyright information, consult the AMS Copyright Policy (www.ametsoc.org/PUBSReuseLicenses).

(see the [appendix](#)) and found that the surface warming in their dataset was actually stronger in the *second*, rather than in the first, posteruption winter. This is difficult to reconcile with the simple fact that the amount of aerosol left in the atmosphere 2 years after an eruption is considerably smaller than in the first year and that the stratospheric circulation possesses no memory from 1 year to the next.

On the modeling side, the results reported in the last decade have proven even more puzzling. With only a couple of exceptions (e.g., [Zambri and Robock 2016](#)), nearly all recent studies have consistently found that state-of-the-art models simulate no significant forced boreal winter warming following the Pinatubo eruption. For instance, [Bittner \(2015\)](#) reported no statistically significant forced Eurasian warming in the first post-Pinatubo winter after averaging over 100 simulations¹ from the Max Planck Institute Grand Ensemble ([Maher et al. 2019](#)). Similar conclusions were reported in [Thomas et al. \(2009a,b\)](#), [Driscoll et al. \(2012\)](#), [Toohey et al. \(2014\)](#), and [Wunderlich and Mitchell \(2017\)](#). The widespread disappearance of the expected posteruption forced warming in the more recent models even led some authors to “raise concern for the ability of current climate models to simulate the response of a major mode of global circulation variability to external forcings” ([Driscoll et al. 2012](#)).

A resolution to this conundrum was proposed by [Polvani et al. \(2019\)](#). Analyzing three large ensembles of state-of-the-art models, they first reported that no forced post-Pinatubo warming in the Eurasian winter was present in those models, in agreement with the findings of most previous studies. Subsequently, examining individual members in each ensemble, they noted that many members simulate Eurasian warming comparable to and even larger than the one observed in the first winter after the Pinatubo eruption; moreover, they noted that many members simulate large posteruption winter cooling when forced with identical aerosols. [Polvani et al. \(2019\)](#) thus concluded that state-of-the-art models are perfectly capable of capturing the winter warming that was observed following the Pinatubo eruption and, more importantly, inferred that the observed post-Pinatubo winter warming—in all likelihood—was nothing more than internal (i.e., unforced) variability and was not caused by the volcanic aerosols.

To explore the generality of that conclusion, [Polvani and Camargo \(2020\)](#) then investigated the Krakatau eruption of August 1883. That event is the only other large, low-latitude eruption in the instrumental period, allowing the posteruption

Eurasian winter temperature anomalies to be estimated from direct observations. Examining three different temperature products derived from observations, [Polvani and Camargo \(2020\)](#) showed that the Eurasian winter temperatures were again anomalously warm in the first post-Krakatau boreal winter but highlighted the fact that those anomalies only fell between 1σ and 2σ of the unforced natural variability (as in the case of Pinatubo). Hence, without the use of any models, they argued that the first post-Krakatau boreal winter warming was unexceptional because many Eurasian winters in the instrumental record exhibit larger warming without a preceding summer eruption. Also, confirming the findings from the 1991 Pinatubo eruption, they found no statistically significant forced boreal winter temperature response in the first post-Krakatau winter in over 40 state-of-the-art models.

Taken together, these recent modeling studies cast considerable doubt on the ability of large, low-latitude eruptions to cause Eurasian winter warming anomalies that stand out from internal variability. If indeed the stratospheric pathway is operative at all, the next step is to consider eruptions larger than Krakatau or Pinatubo. On the modeling front, two studies have explored such events.

In the first study, [Azoulay et al. \(2021\)](#) performed and analyzed 100-member ensembles of simulations with a stratospheric-resolving model, exploring stratospheric injection amplitudes ranging² from 2.5 to 20 Tg(S). First, they confirmed the absence of any statistically significant Eurasian winter warming when the model was forced with Pinatubo aerosols. Second, they reported small, yet statistically significant, forced winter warming over some regions of northern Eurasia with sufficiently large eruptions using synthetic aerosols from the Easy Volcanic Aerosol (EVA) protocol ([Toohey et al. 2016](#)). They found the threshold for significance³ to be at 10 Tg(S) and a forced winter warming of about of 1°C over Scandinavia and northern Eurasia.

In the second study, [DallaSanta and Polvani \(2022\)](#) independently confirmed these results. Using a different stratosphere-resolving model, they performed and analyzed smaller 20-member ensembles with the same EVA aerosols, but explored a larger range of stratospheric injections, progressively doubling the injection mass from 5 to 160 Tg(S). They also found small yet statistically significant warming over parts of Eurasia in the first posteruption winter in their model, with the threshold at 20 Tg(S). However, they emphasized two additional aspects. First, they noted that a large number of eruptions is needed to establish statistical significance: for instance, for a 40-Tg(S) injection—which is larger than all but one of the eruptions that are known to have occurred in the last millennium (LM; see [Table 1](#))—eight or more eruptions

¹ It is important to appreciate how the early model used by [Graft et al. \(1993\)](#) compares with the more recent one used by [Bittner et al. \(2016\)](#). The latter is a stratosphere-resolving atmospheric model, with 47 vertical levels and a model top at 0.01 hPa, interactively coupled to ocean, land, and sea ice components and forced with realistic volcanic aerosol distributions that are then passed on to the radiative transfer scheme. The former was an atmosphere-only model, with only 19 vertical levels and a low model top at 10 hPa, run under perpetual January conditions (i.e., without a seasonal cycle), with prescribed sea surface temperatures and sea ice concentrations, and only forced with an externally computed heating rate but without any actual volcanic aerosols in the model itself.

² As a point of reference, Pinatubo and Krakatau resulted in injections of 8.78 and 9.34 Tg(S), respectively, according to the latest estimate ([TS17](#)). See [Table A1](#).

³ This threshold value is only a little larger than the Pinatubo and Krakatau estimates of sulfur injection mass, but the EVA aerosols produce a stronger forcing so that, with a 100-member ensemble, a small but statistically significant surface response can be established.

TABLE 1. The 20 tropical volcanic eruptions greater in magnitude than Pinatubo 1991, from the eVolv2k_v2 database (TS17), ordered chronologically. The unknown month, day, or latitude (within the tropics) of the eruption is indicated as “—”. The symbol “-/-” is used to indicate that there are no dating uncertainties in the year of the event. The σ indicates the uncertainty. Asterisks denote the eruptions occurring after 1500. This set of 20 eruptions is referred to as TVE_{ev}.

Name	Year	Year (σ)	Month	Day	VSSI (TgS)	VSSI (σ)	Latitude (°)
*Krakatau	1883	-/-	8	27	9.34	1.91	-6
*Cosigüina	1835	-/-	1	20	9.48	2.21	13
*Babuyan Claro	1831	± 1	—	—	12.98	3.41	19.5
*Tambora	1815	-/-	4	10	28.08	4.49	-8
*Unknown	1809	-/-	—	—	19.26	3.54	—
*Unknown	1695	± 1	—	—	15.74	2.88	—
*Parker	1640	-/-	w	26	18.68	4.28	6.1
*Huaynaputina	1600	-/-	2	17	18.95	4.03	-16.6
*Nevado del Ruiz	1595	-/-	3	9	8.87	1.51	4.9
*Colima	1585	-/-	1	10	8.51	2.34	19.5
Unknown	1458	± 1	—	—	32.98	4.8	—
Kuwa	1453	± 1	—	—	9.97	3.07	—
Unknown	1345	-/-	—	—	15.11	2.86	—
Unknown	1286	± 1	—	—	15.06	2.79	—
Unknown	1276	-/-	—	—	11.53	1.63	—
Samalas	1257	-/-	7	—	59.42	10.86	-8.4
Unknown	1230	± 1	—	—	23.78	5.24	—
Unknown	1191	-/-	—	—	8.53	1.49	—
Unknown	1171	± 1	—	—	18.05	3.67	—
Unknown	1108	± 1	—	—	19.16	4.71	—

are needed to establish significance (and many more for smaller mass injections). Second, they reported that the forced winter warming over Eurasia, for up to 80-Tg(S) eruptions, is smaller than one standard deviation of the internal year-to-year variability of Eurasian winter temperatures. They thus concluded that even for the very largest eruptions over the LM, any post-eruption winter warming anomalies would be largely unremarkable over Eurasia.

These two modeling studies offer a hint that while Pinatubo or Krakatau may not be sufficiently strong, perhaps even larger low-latitude eruptions might be able to produce some observable winter warming over Eurasia. Hence, the goal of this paper is to reexamine the paleoclimatic record over the LM in light of the most recent modeling work. Seeking evidence for posteruption Eurasian winter warming (presumably via the stratospheric pathway), we have produced a new temperature reconstruction over the LM specifically designed for this purpose by assimilating temperature observations and retaining only those proxies that have sensitivity in the winter months [December–February (DJF)]. With this new reconstruction, we then examine the largest 20 low-latitude eruptions of the LM. As detailed below, we find that 13 of those 20 events show Eurasian surface cooling in the first posteruption winter, which stands in sharp contrast to the claims made in most of the earlier literature, notably the study of Fischer et al. (2007) who concluded that eruptions are followed by winter warming over Europe.

The paper is laid out as follows: In section 2, we describe how the new surface temperature reconstruction was obtained and validated, how the analyzed eruptions were chosen, and how the temperature anomalies were computed. The key results are then presented in section 3, where the new

posteruption boreal winter temperature anomalies for each of the LM events are individually shown in the context of the unforced variability over Eurasia. In section 4, we reexamine the earlier literature, notably the seminal study of Robock and Mao (1992), the study of Fischer et al. (2007), and the recent reconstruction of Eurasian winters by Reichen et al. (2022). We demonstrate how methodological issues and, in particular, the widespread—and often inappropriate—averaging of large and small eruptions, have been at the root of the earlier claims of a forced posteruption winter warming, which we herein show is not supported by paleoclimatic estimates. We conclude with a summary and discussion.

2. Data and methods

a. The new Winter Temperature Eurasian Data Assimilation (WinTEDA) reconstruction

Our new paleo data assimilation temperature reconstruction—called WinTEDA—is based on the same methodology used for the Paleo Hydrodynamics Data Assimilation (PHYDA) product (Steiger et al. 2018) but with two key differences. First, in WinTEDA, we also include instrumental observations in the assimilation process. Second, in WinTEDA, we only include proxies with DJF sensitivities.

WinTEDA was built as follows: We retrieved long instrumental data from the Berkeley Earth Observatory repository (Rohde and Hausfather 2020) and individual stations and selected only those stations (a total of 367) that contained data prior to 1850 and at least 10 years of continuous data. We combined that information with 365 Eurasian high-resolution paleoclimatic proxy time series, comprising 340 tree-ring series and 25 ice core records, shown in Fig. 1a. Even though

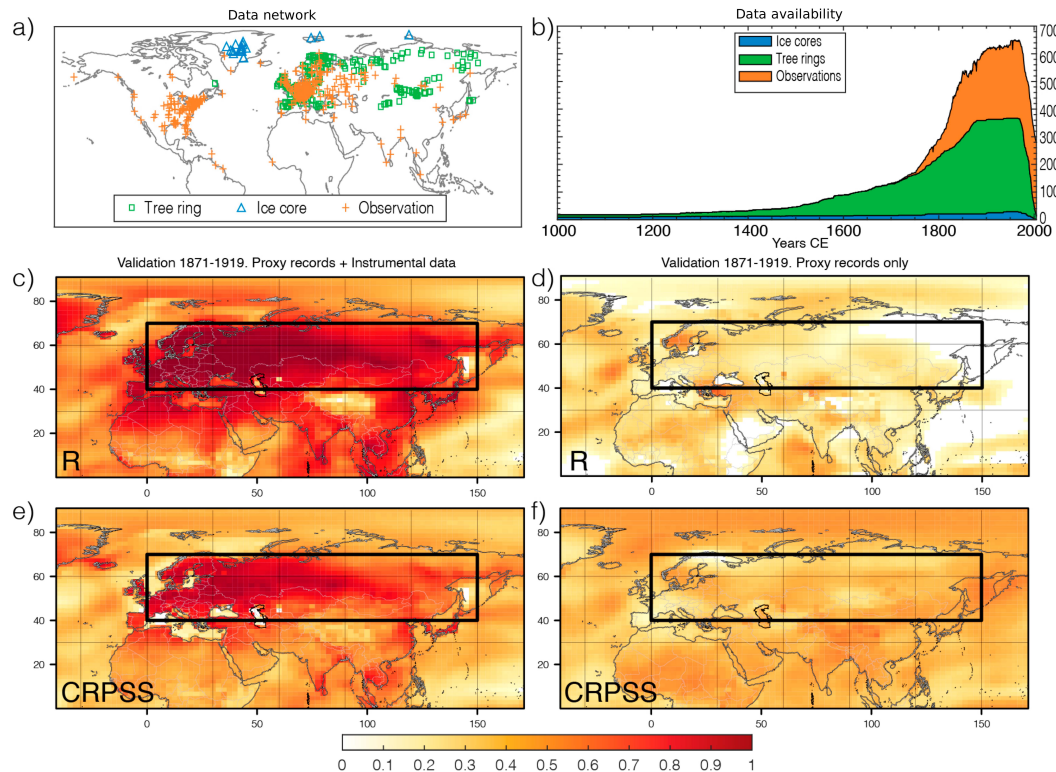


FIG. 1. The new data assimilation product (WinTEDA), targeting DJF temperature over Eurasia. (a) Network of proxy and long instrumental records used in WinTEDA. (b) Data availability over the LM. (c) Pearson's correlation for each of the reconstructed grid points and the Berkeley Earth instrumental data for DJF temperature at 2 m over the validation period (1871–1919, i.e., the calibration period 1920–2000 is not shown), including both the proxy and the instrumental data. (d) As in (c), but for including only proxy data. (e),(f) As in (c),(d), but for the CRPSS.

many more proxy records are available over Eurasia, we selected only those proxies with DJF sensitivity, specifically with a significant ($p < 0.05$) correlation with the Berkeley Earth Observatory instrumental data in DJF over the 1920–2000 calibration period. Additionally, following the application of a dual detrending process to eliminate nonclimatic signals from the trees, we rely on the resulting residual chronology to examine year-to-year high-frequency variability, which aligns with the specific focus of our study and avoids the potential memory effect seen in tree-ring width records (e.g., Tejedor et al. 2021a). The data assimilation method was subsequently applied by including the physical constraints of an atmosphere–ocean climate model simulation (in this case, we used the CESM-Last Millennium Ensemble Project (CESM-LME) simulation number 10; Otto-Bliesner et al. 2016) to develop the DJF temperature reconstruction. The data assimilation approach is naturally probabilistic and provides an ensemble of equally likely reconstructions. For this paper, we analyze a random sampling of 100 members from the original 998 (as in PHYDA). Because of the way in which the reconstructions are done, the ensemble does not necessarily provide the uncertainties in the traditional way. Instead, it provides the mean of the spread across the different members.

We have confined our analysis to the period 1000–1900 CE, as the proxy availability prior to 1000 CE is very limited (see Fig. 1b). We specifically targeted the boreal winter season (December–February) near-surface temperature, which was reconstructed on a 2° latitude–longitude grid (following the resolution of the model simulation). We calculated the temperature anomalies in degrees Celsius with respect to 1000–1900 CE. Finally, we use the year of December month to label the WinTEDA temperature reconstruction, e.g., the WinTEDA year 1600 temperature is the average of December 1600 and January–February 1601.

To assess the quality of our reconstruction, we computed several metrics for the verification period (1871–1919). For each grid point, we first validated the reconstruction by computing both the coefficient of efficiency (CE; Nash and Sutcliffe 1970) and the point-by-point Pearson's correlations between each of the grid cells and the nearest station of the Berkeley Earth Observatory instrumental data. The WinTEDA skill is especially good for western Europe, including CE values > 0.8 (not shown) and high Pearson's correlations ($r > 0.7$, $p < 0.05$; Fig. 1c), with easternmost Siberia displaying the lowest estimates, although still presenting skillful metrics. We then computed the continuous ranked probability score (CRPS): this measures the difference between the WinTEDA and the observed values. Then, we calculated the continuous

ranked probability skill score (CRPSS): this is the reconstructed CRPS computed with respect to the CRPS of a reference distribution (i.e., $\text{CRPSS} \equiv 1 - \text{CRPS}_{\text{rec}}/\text{CRPS}_{\text{ref}}$), here chosen to be the initial uninformed CESM climate model simulation. We use CRPSS instead of CRPS because CRPS has the referenceless range of (0 to ∞), while CRPSS has the range ($-\infty$ to 1). Recall that a positive CRPSS indicates that the reconstruction is more skillful than the uninformed prior. As shown in Figs. 1c and 1e, WinTEDA shows overall good reconstruction skill over Eurasia, with a mean CRPSS of ~ 0.8 over that region for the validation period (1871–1919 CE). Such high skill measures are somewhat expected given that we included instrumental records in the assimilation method. To address this consideration, we present the performance of the reconstruction using only proxies within the calibration period from 1920 to 2000 CE (see Figs. 1d,f, where only the validation results over the period 1871–1919 CE are shown). While the reconstruction's performance is naturally reduced after dropping instrumental data, Figs. 1d and 1f clearly indicate a skillful reconstruction, particularly for the period prior to the mid-seventeenth century when instrumental data are unavailable.

Finally, it is important to note that WinTEDA was constructed as an offline data assimilation product. An important implication of this approach is that while the model simulation that was incorporated as the prior has explicit temporal histories tied to the prescribed forcing in the model, the temporal information is not incorporated in the data assimilation methodology, i.e., the timing of climate events such as volcanic eruptions or trends over specific periods (e.g., twentieth century warming) is not dictated by the prior. Consequently, all temporal structure in WinTEDA is tied specifically to the information contained in the assimilated observational and proxy networks (Steiger et al. 2018; Tardif et al. 2019).

While we believe that WinTEDA is a reliable reconstruction that allows us to explore the climatic effects of large volcanic eruptions over the entire LM, in sections 4b and 4c, we carefully compare WinTEDA to two other winter reconstructions. The first one was used in the Fischer et al. (2007, hereafter F07) study that reported posteruption winter warming over Europe (Luterbacher et al. 2004). The second, referred to as EKF400_v2 (Valler et al. 2022), is a global data assimilation product that includes proxies and observational instrumental temperature and pressure data. As we show below, for the boreal winters following large eruptions, WinTEDA is in good agreement with these two other reconstructions.

b. Last millennium volcanic data

As reviewed in the introduction, two key ingredients are important for an eruption to produce a detectable surface impact over Eurasia via the stratospheric pathway: first, the eruption must produce a large stratospheric injection and second, that injection must occur at low latitudes. There is now ample evidence that eruptions as large as Pinatubo (1991) are simply not strong enough to produce a detectable surface impact via the stratospheric pathway mechanism. We therefore confine our analysis herein to those low-latitude eruptions over the LM that are larger than Pinatubo.

To identify such events, we employ the most recent global volcanic forcing reconstruction database, called eVolv2k_v3 [Toohey and Sigl 2017 (hereafter TS17), 2019], which is based on a suite of ice core records from Greenland and Antarctica. This database reports estimates of source latitude and magnitude [in terms of volcanic stratospheric sulfur injection (VSSI)] for all major events from 500 BCE to 1900 CE. The eVolv2k_v3 database represents a significant advancement over prior estimates that relied on volcanic forcing reconstructions with greater chronological uncertainty (Crowley and Unterman 2013; Gao et al. 2008). Accurately selected eruption dates are crucial for resolving subannual to annual volcanic responses in the proxy data and for detecting the potential posteruption boreal winter warming over Eurasia (see Zhu et al. 2022 for a cautionary tale about the importance of selecting events when the sample size is relatively small).

In eVolv2k_v3, we find 20 low-latitude eruptions larger than Pinatubo (i.e., with $\text{VSSI} > 8.78 \text{ Tg S}$) over the period covered by WinTEDA (1000–1900 CE). Their names (when known) and properties are listed in Table 1; for consistency, we will refer to this set as the “tropical volcanic events from eVolv2K_v3” (TVE_{ev}). The largest event in this set is the Samalas eruption of 1257, with a VSSI near 60 Tg(S) , followed by an unknown event in 1458 with a VSSI of 33 Tg(S) , followed by the well-documented Tambora eruption of 1815 at 28 Tg(S) . Except for Samalas, these eruptions are at most a few times as large as Pinatubo in terms of VSSI, but with a total of 20 events, one would hope that TVE_{ev} should allow detection of a winter surface impact over Eurasia if a robust forced response exists.

c. Analysis methods

We focus our paper on the *first* DJF winter following each eruption. There has been much confusion about this in the earlier literature, with papers considering both the first and the second winter (e.g., F07) or a mixture of the two (e.g., Robock and Mao 1992). In recent years, a consensus has emerged that only the first posteruption winter should be examined (e.g., Zambri and Robock 2016; Polvani et al. 2019; Azoulay et al. 2021), as there is no memory in the stratosphere that would persist beyond the first posteruption winter. Nonetheless, due to uncertainties in the dating of several eruptions in the LM, we also briefly examine the second posteruption winter to ensure that our conclusions are robust.

We define the surface temperature anomalies as the difference between a given boreal winter and the mean of the previous five winters (the reference period). This definition follows Polvani et al. (2019) and has been shown to be robust to the length of the averaging period (Polvani and Camargo 2020). In some earlier studies (Stenchikov et al. 2006; Driscoll et al. 2012), reference periods of different lengths were chosen for different eruptions. We believe this to be an inferior choice, as the impact of different eruptions is thereby quantified with different metrics. We also note that the anomalies in many modeling studies (e.g., Azoulay et al. 2021) are not defined as we do here. Rather, they are defined as the difference from a control integration with identical initial conditions but

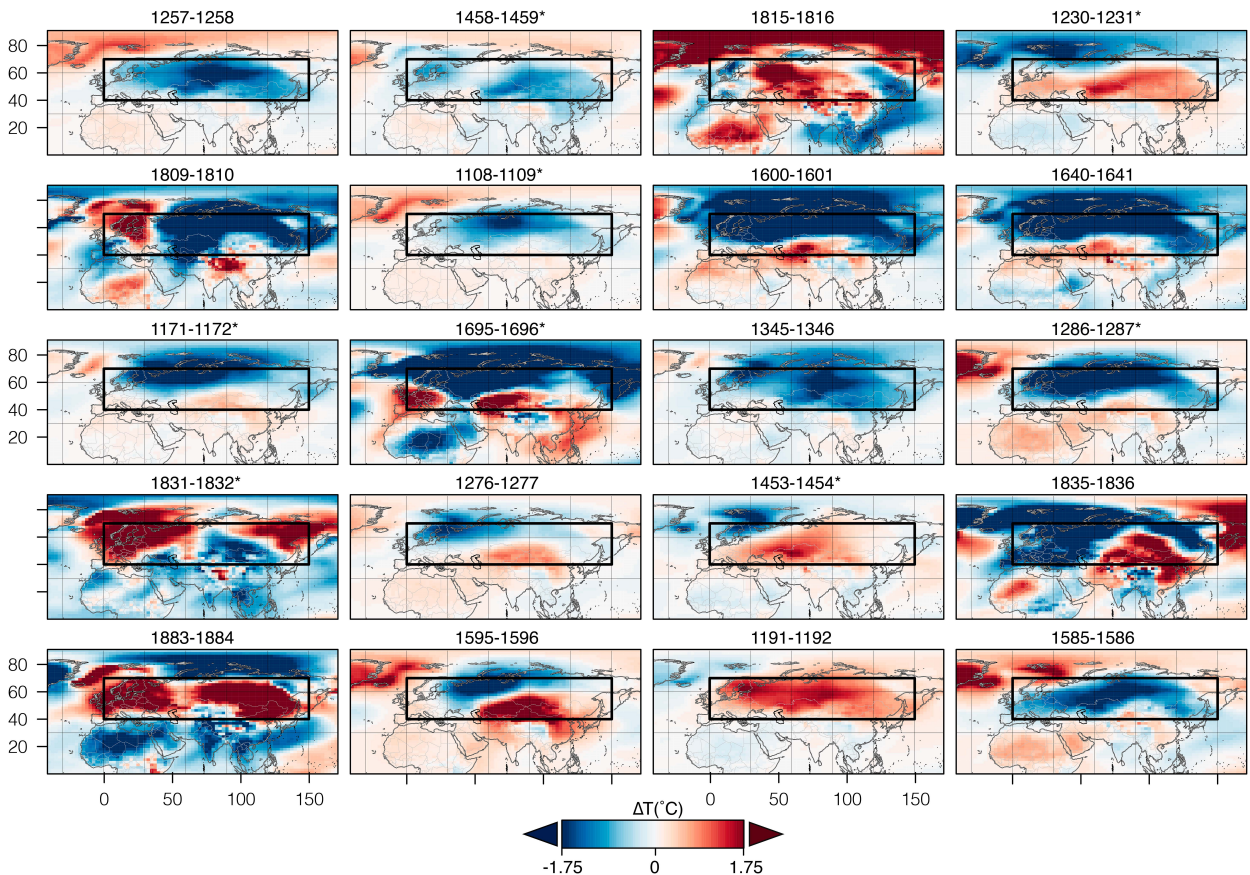


FIG. 2. Ensemble mean surface temperature anomalies in the WinTEDA reconstruction, for the first winter (DJF) following the 20 eruptions in TVE_{ev} (see Table 1; the readers who fear a warming signal might be lurking in the second posteruption winter will be reassured after consulting the appendix). The events are shown in order of decreasing VSSI. Asterisks denote events with dating uncertainties. The box over Eurasia, as in Polvani et al. (2019), is used for computing the Eurasian mean values.

with no eruption. As shown in DallaSanta and Polvani (2022), these two methods yield comparable answers. However, the second method cannot be used to analyze observations or reconstructions—hence our choice.

Finally, we will present many maps of temperature anomalies over the entire Northern Hemisphere, but in several figures, we synthesize the results with a single number by averaging over a simple latitude–longitude box covering the bulk of Eurasia. Following Polvani et al. (2019), we use the region from 40° to 70°N and from 0° to 140°E to define this box. While there is some small sensitivity to the choice of the averaging region (Azoulay et al. 2021; DallaSanta and Polvani 2022), the key conclusions of our study are robust across a range of choices.

3. Posteruption Eurasian surface temperature anomalies in the context of internal variability

a. Posteruption winter temperature anomalies

The key result of our study is presented in Fig. 2, where the surface temperature anomalies in the first posteruption winter over Eurasia are shown for each of the 20 events in TVE_{ev} (Table 1). In contrast to the posteruption warming as reported

in much of the previous literature, we find that 13 out of 20 of the selected events are followed by a winter cooling over the Eurasian box. This cooling is especially prominent for the boreal winters of 1600/01, 1695/96, 1640/41, 1809/10, and 1286/87, with anomalies in excess of -1°C . Interestingly, we also find a number of posteruption winters with warm anomalies: the largest of these is found to be the boreal winter of 1883/84, immediately following the Krakatau eruption of August 1883, with a Eurasian mean warming of 1.7°C , in good agreement with the instrumental values reported by Polvani and Camargo (2020; see their Fig. 3).

As Fig. 2 only shows the ensemble mean anomalies for each event, in Fig. 3, we present the entire distribution of the posteruption Eurasian wintertime anomalies across all 100 WinTEDA members, for each of the 20 eruptions in TVE_{ev} , with blue/red filled boxplots (the green empty boxplots are discussed later in section 4c). Note that these distributions show the variance across ensemble members for each eruption, which is not strictly the uncertainty, because much of the spread of the ensemble has been removed by the compositing process. Thus, the boxplot distributions tend to have larger variance when more proxy and observational data inform the reconstruction (with decreasing information, the data assimilation process

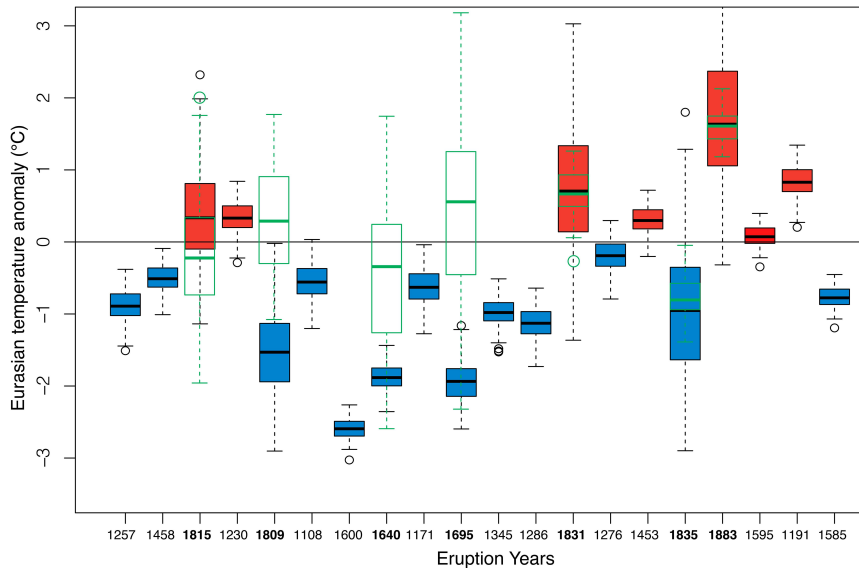


FIG. 3. Distributions of posteruption surface temperature anomalies in the first winter (DJF) following each of the 20 eruptions in TVE_{ev}, averaged over the Eurasian box shown in Fig. 2. For each event, labeled by the year of occurrence on the abscissa, a black box-and-whisker plot summarizes the distribution of the 100 WinTEDA members. For the 7 events after 1600, green boxplots show the EKF400_v2 anomalies (30 members). Filled boxplots are for WinTEDA, and empty boxplots are for EKF400_v2. In each boxplot, the dark line shows the median, the edges of the boxes are 25th and 75th percentiles, the whiskers extend to 1.5 standard deviations above or below the median, and the outliers are shown in circles. Events are sorted, left to right, by decreasing VSSI. Bold years highlight events with both datasets available.

tends to increasingly favor the prior ensemble and thus reduce the reconstructed mean variance). This explains why the spreads in Fig. 3 appear larger for the post-1800 eruptions than for the earlier ones. The absence of instrumental data for the oldest eruptions makes them appear less uncertain than the most recent ones, but of course, this is unlikely to be the case.

With this in mind, it is instructive to note that some eruptions show a wide range of possible temperature anomalies. Consider, for instance, the large Cosigüina eruption of 1835: although the median value is approximately -1.0°C , some ensemble members show a cooling as large as -2.8°C , while many members show a posteruption warming as large as 1.8°C . Alternatively, consider the event with the largest median warming, the Krakatau eruption of 1883, and note that some members of the reconstruction ensemble show cooling. This is not a flaw in the WinTEDA reconstruction but reflects intrinsic uncertainties associated with observational estimates of the eruption response over Eurasia: Polvani and Camargo (2020) analyzed that same eruption with a 56-member ensemble of the twentieth century reanalysis (Compo 2011) and also reported that while the ensemble mean showed warming, several members of that reanalysis showed post-Krakatau cooling. Most previous studies dealing with the climatic effect of volcanic eruptions, however, have largely failed to highlight the small value of the signal-to-noise ratio.

It is important to note that although we have plotted the eruptions in decreasing order of amplitude (in terms of VSSI), the cooling shown by the blue bars in Fig. 3 does not

monotonically decrease from left to right. In fact, the correlation coefficient between posteruption winter Eurasian cooling and VSSI is small and insignificant ($r = -0.19$, $p < 0.414$). Considering specific events, the third and fourth largest events (1815 and 1230) show posteruption winter warming, while the two largest events show cooling. Conversely, the three coldest posteruption winters in WinTEDA—occurred in 1600/01, 1695/96, and 1640/41—correspond to eruptions with a VSSI of approximately 19, 16, and 19 Tg(S), which are not the three largest eruptions of the LM, and are barely twice the amplitude of the 1991 Pinatubo eruption. These examples illustrate that the signal-to-noise challenge is daunting.

With the above results in mind, we now ask: what can one actually conclude from Fig. 3? We highlight several facts in this regard. First, 13 of 20 eruptions show Eurasian winter cooling in the ensemble mean, larger than -1.0°C for seven events. Second, in each of the events with an ensemble mean warming, one or more ensemble members show cooling. In contrast, for 10 of 13 events with ensemble mean cooling, none of the ensemble members show warming. Third, lumping all eruptions and all ensemble members in a single sample (of size 2000), we find that over the LM, a large, low-latitude volcanic eruption is followed by an anomalously cold Eurasian winter 68.4% of the time. Taken together, we claim that the WinTEDA reconstruction leads us to conclude there is simply no evidence that large, low-latitude volcanic eruptions cause winter warming over Eurasia.

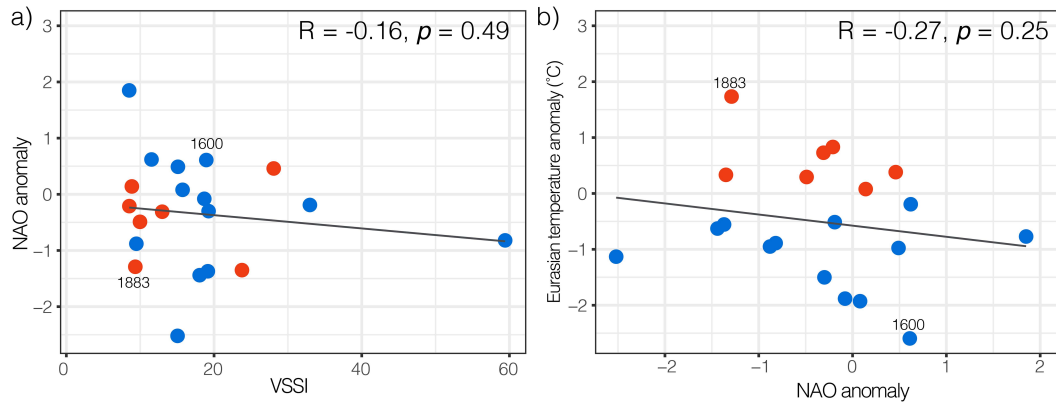


FIG. 4. Scatterplots between (a) the NAO index and VSSI and (b) Eurasian surface temperature and the NAO index, in the first winter after the 20 volcanic eruptions in the LM (TVE_{ev}). Blue/red dots show the years with posteruption Eurasian winter cooling/warming (averaged over the boxes shown in Fig. 3). Warmest (1883) and coolest (1600) posteruption winters are highlighted. Regression lines are shown in black; associated Spearman's rank correlation coefficients, and p values, are shown in the top-right corner of each panel.

To corroborate this conclusion, we also examined whether any evidence exists in support of the stratospheric pathway mechanism. There are no observations of the state of the stratosphere hundreds of years ago, but because the stratospheric polar vortex is known to impact surface conditions via the NAO (e.g., Baldwin and Dunkerton 2001), we have analyzed one NAO reconstruction (Cook et al. 2019) seeking evidence of the stratospheric pathway. First, we examined the entire NAO time series over the LM and found a small but statistically significant correlation between that NAO reconstruction and the WinTEDA Eurasian winter surface temperature ($r = 0.20$, $p < 0.01$, $n = 1000$). We then examined the 20 posteruption winters: as one can see in Fig. 4, there is no correlation between the NAO anomalies and the VSSI in the posteruption winter, nor is there one between the Eurasian mean temperature and the NAO anomalies. Recall that most recent modeling studies (Azoulay et al. 2021; DallaSanta and Polvani 2022) have shown that 20 events may not be sufficient to establish a statistically significant NAO response (should one actually exist) to the volcanic aerosols. Our WinTEDA analysis is consistent with these modeling results.

We also add that the lack of correlation between the amplitude of the volcanic eruptions and the winter NAO seen in Fig. 4a confirms the findings of Osman et al. (2021), who also found no linkage between the North Atlantic jet and volcanic eruptions over the past 1250 years. That study, incidentally, contradicts the earlier findings of Ortega et al. (2015), who analyzed a new NAO reconstruction over the LM and claimed that a positive NAO anomaly emerges in the second posteruption winter. The very fact that two papers can be found in the extant literature reporting diametrically opposite claims speaks volumes as to the lack of robustness of the proposed stratospheric pathway mechanism.

Finally, leaving aside the question of which specific physical mechanism may or may not be responsible for the posteruption anomalies, we ask a simpler—yet more important—question: are the winters following the 20 largest, low-latitude

eruptions of the LM exceptional in some way? In other words, are they noticeably different from the winters that do not follow a large eruption? To answer that question, we examine the posteruption winter temperature anomalies in the context of all winter temperature anomalies over Eurasia in Fig. 5.

The boreal winter temperature distribution, computed from the nearly 1000 WinTEDA winters at our disposal (minus the 20 posteruption winters), is shown by the black curve in Fig. 5. Note that the 2σ range is approximately $\pm 2^\circ\text{C}$, in good agreement with the values reported by Polvani and Camargo (2020) over the shorter instrumental period (from roughly 1850 to present). What is immediately clear from Fig. 5 is that most of the surface temperature anomalies

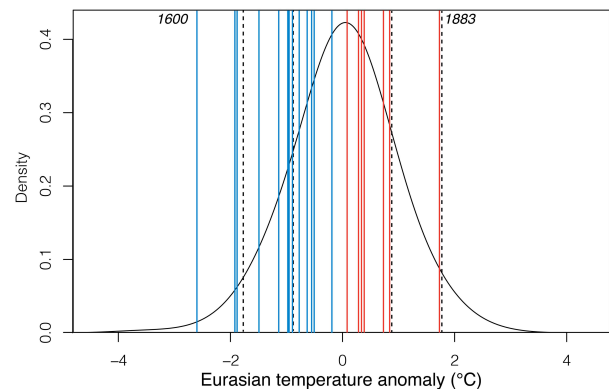


FIG. 5. Winter (DJF) surface temperature anomalies averaged over the Eurasian box shown in Fig. 2. Black line: distribution for all winters over the preindustrial LM (1000–1900 CE) but excluding the 20 TVE_{ev} winters, with the black dashed lines showing the $\pm 1\sigma$ and $\pm 2\sigma$ ranges. A nonparametric kernel density estimator was used to visualize the density distribution. Colored lines: the 20 posteruption winters, averaged over the 100-member WinTEDA ensemble: blue for the anomalously cold winters and red for the warm winters. Labels at the top indicate the warmest and coolest winters following TVE_{ev} , respectively.

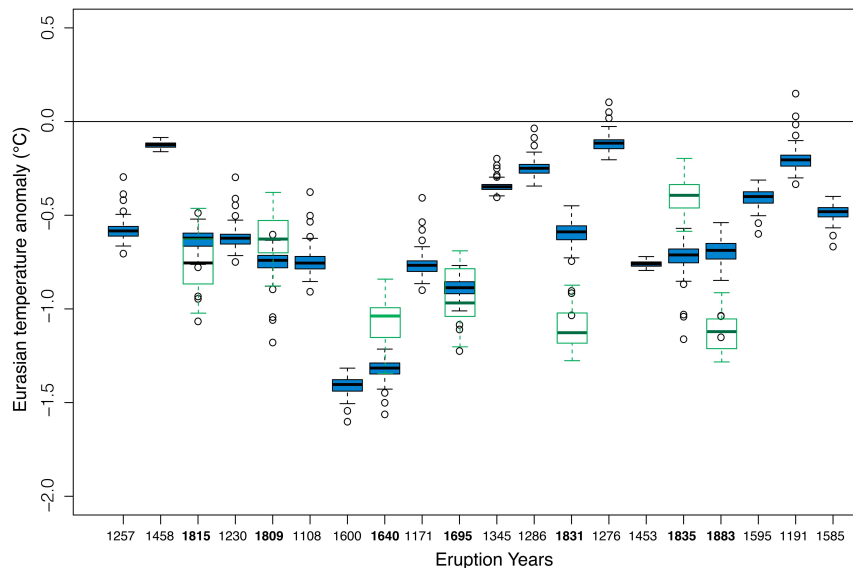


FIG. 6. As in Fig. 4, but for summer (JJA) and using PHYDA (Steiger et al. 2018). Green empty boxplots show the EKF400_v2. Bold years indicate events present in both datasets.

following the 20 largest eruptions of the LM (the colored bars) are within the 2σ range of the all-winters distribution and thus unremarkable. Specifically, only 3 of the 20 events fall outside the 2σ range (all cold anomalies) and only 10 of 20 fall outside the 1σ range (all cold anomalies except for one). The clear message from Fig. 5 is that, based on surface temperature anomalies alone, one would be unable to distinguish the posteruption boreal winters from the rest.

b. Posteruption summer temperature anomalies

Although the stratospheric pathway is not operative in the summer (June–August) months, as the polar vortex disappears in the spring, it is nonetheless instructive to examine the posteruption summer temperatures over Eurasia. To do this, we analyze the original PHYDA reconstruction (Steiger et al. 2018) because it incorporates a much larger network of proxies than WinTEDA and because it was created to target the summer growing season. For each of the 20 eruptions in TVE_{ev} , the 100-member ensemble of PHYDA anomalies in JJA are shown in Fig. 6. For all 20 events, the ensemble means show cooling. In fact, except for three members for the 1276 event and for an additional two members for the 1191 event, the remaining 995 (of the total 2000) members across all 20 eruptions show summer cooling.

More importantly, we emphasize that even in boreal summer, the posteruption cooling anomalies need to be considered in the context of those arising from internal variability alone. As for the winter season, we find little correlation between the magnitude of the summer cooling and the VSSI ($r = 0.2$), again indicating a considerable role for internal variability, which obscures the expected link between VSSI magnitude and surface cooling. Nonetheless, as shown in Fig. 7, we find that 12 events exceed the 2σ range in summer, with two events larger than 4σ : this is a

clear indication of a forced cooling response to the eruption emerging in the boreal summer months.

4. Reconciling our finding with previous studies

The key finding of our study—the lack of evidence for a winter warming in Eurasia following large, low-latitude volcanic eruptions—is at odds with the findings reported by nearly all previous studies on this subject, which have consistently argued that such winters are anomalously warm. It is imperative, therefore, that we explain how previous studies reached a different conclusion. We have no room for an exhaustive discussion of all previous studies, so we have decided to focus primarily on the most recent and comprehensive⁴ paleoclimatic study (F07) to explain in detail how their conclusion was arrived at and why it differs from ours. We also repeat our analysis with another recent temperature reconstruction (Valler et al. 2022; Reichen et al. 2022) to corroborate our findings. Before doing so, however, we briefly reexamine the seminal study of Robock and Mao (1992) and other early studies to illustrate the history of the postvolcanic boreal winter warming claim and the weak foundations on which it was built.

a. Robock and Mao (1992) and other early studies

Following an early suggestion by Groisman (1992), Robock and Mao (1992) first proposed the winter warming idea in the wake of the large 1991 Mount Pinatubo eruption. Their analysis focused on a dozen eruptions from 1883 to 1991, and we

⁴ We here confine our discussion to observational studies alone, i.e., those based on temperature reconstructions. There is a much larger body of modeling studies. For a review of those, we refer the reader to the discussion sections in Polvani et al. (2019) and DallaSanta and Polvani (2022).

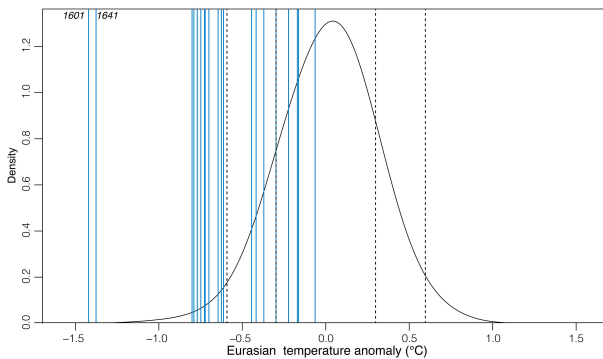


FIG. 7. As in Fig. 5, but for summer (JJA).

highlight three issues that we find particularly problematic. First, of the 12 eruptions examined by Robock and Mao (1992), six occurred at midlatitudes: for those events, a stratospheric pathway is unlikely to be operative, as the volcanic aerosols are unable to force an anomalous equator-to-pole temperature gradient in the stratosphere. Second, the first posteruption boreal winter was analyzed by Robock and Mao (1992) for the low-latitude events, but for the high-latitude eruptions, the second winter was used. There is no clear justification for this choice given that there is no memory in the stratosphere⁵ from one winter to the next. Third, and most importantly, other than 1991 Pinatubo and 1883 Krakatau (and 1912 Katmai, at a latitude of 58°N), all other eruptions analyzed in Robock and Mao (1992) are associated with small events (<8 Tg S). Given the relatively small expected magnitude of the forced responses and the very large internal variability of midlatitude continental winter temperatures, averaging a couple of large events with many smaller events contaminates a possible small signal with a lot of noise.

A subsequent study by Robock and Mao (1995) suffers from similar issues, which are aggravated by the addition of two eruptions at high latitudes [Askja (in 1875) located at 65°N and Mount Saint Helens (in 1980) located at 46°N]. These two early studies were highly influential and were followed by later efforts that, while attempting to provide additional evidence for a Eurasian posteruption winter warming, in fact reached conclusions that were couched in very cautious language. For instance, Kelly et al. (1996) analyzed only five events and reported “a limited high latitude warming” adding, however, that “the lack of statistical significance associated with this finding is troubling.” Jones et al. (2003) analyzed 15 eruptions using temperature reconstructions going back to the seventeenth century over three regions: central England, Fennoscandia, and central Europe. Again, averaging across high- and low-latitude eruptions and eruptions of different magnitudes, they found no evidence of posteruption winter warming over central England and central Europe; as for Fennoscandia, they reported that their data “indicate slight

warming . . . but the significance level is not reached.” Finally, Shindell et al. (2004) analyzed 18 eruptions dating back to Huaynaputina (1600) and, again averaging over eruptions with disparate magnitudes, reported that “warm anomalies occur throughout northern Eurasia,” yet noted that “the interannual variability is larger than the mean response to volcanic eruptions nearly everywhere.” Furthermore, rather than focusing on DJF alone (when a strong polar vortex is present in the stratosphere), Shindell et al. (2004) analyzed the surface temperature averaged from October to March; this is a problematic choice because there is no stratosphere–troposphere dynamical coupling in October, November, or March, as one can see from Fig. 1a of Baldwin et al. (2003).

b. Fischer et al. (2007)

One common trait of the above studies is a technique known as superposed epoch analysis (SEA; Hegerl et al. 2003), which is very common in the study of the climatic impact of volcanic eruptions. SEA characterizes volcanic impacts by compositing over a set of eruptions and referencing them all to their eruption year as the common year zero. This compositing is done for eruptions based on different criteria, but it is often done for eruptions with vastly different magnitudes. SEA has proven useful in documenting the long-term hydroclimatic (see e.g., Rao et al. 2017; Tejedor et al. 2021a; Anchukaitis et al. 2010) or temperature (e.g., Stoffel et al. 2015; Tejedor et al. 2021b) impacts of volcanic eruptions, which might involve oceanic feedbacks (for example). This technique may be misleading,⁶ however, when addressing the specific issue of Eurasian winter warming, for which the signal-to-noise ratio is likely to be small. As highlighted in Polvani et al. (2019), the volcanic impact we are seeking to characterize is a *forced response* to an external agent; thus, the amplitude of the response is expected to grow with the amplitude of the forcing. Averaging large eruptions, such as Samalas or Tambora, together with much smaller eruptions, as in SEA applications, may therefore significantly obscure the nature of the forced response over specific regions because of the high levels of internal variability. In other words, since the signal-to-noise ratio is small, averaging over eruptions of different sizes dilutes the strong signal of the larger events while adding noise from the smaller ones, hence producing a nonrobust result. We illustrate this explicitly below, as we contrast our findings with those of F07.

Recall that F07 focused on 15 large, low-latitude eruptions over the last half millennium using the Luterbacher et al. (2004, hereafter LUT04) reconstruction. For clarity and reproducibility, those 15 eruptions are listed in Table A1; they include many that we have analyzed in WinTEDA and several smaller ones. Averaging over their 15 eruptions, F07 reported that “in the Northern Hemisphere, winter volcanic forcing induces . . . a significant overall warm anomaly and wetter conditions over Northern Europe.” Surprisingly, this warming—which F07 interpreted as the response to volcanic

⁵ We wish to highlight that *all* recent modeling studies have confined their analysis to the first posteruption winter only. See, for instance, the reasoning of Zambri and Robock (2016).

⁶ For a critique of SEA, in the context of solar cycle impacts, see Haurwitz and Brier (1981).

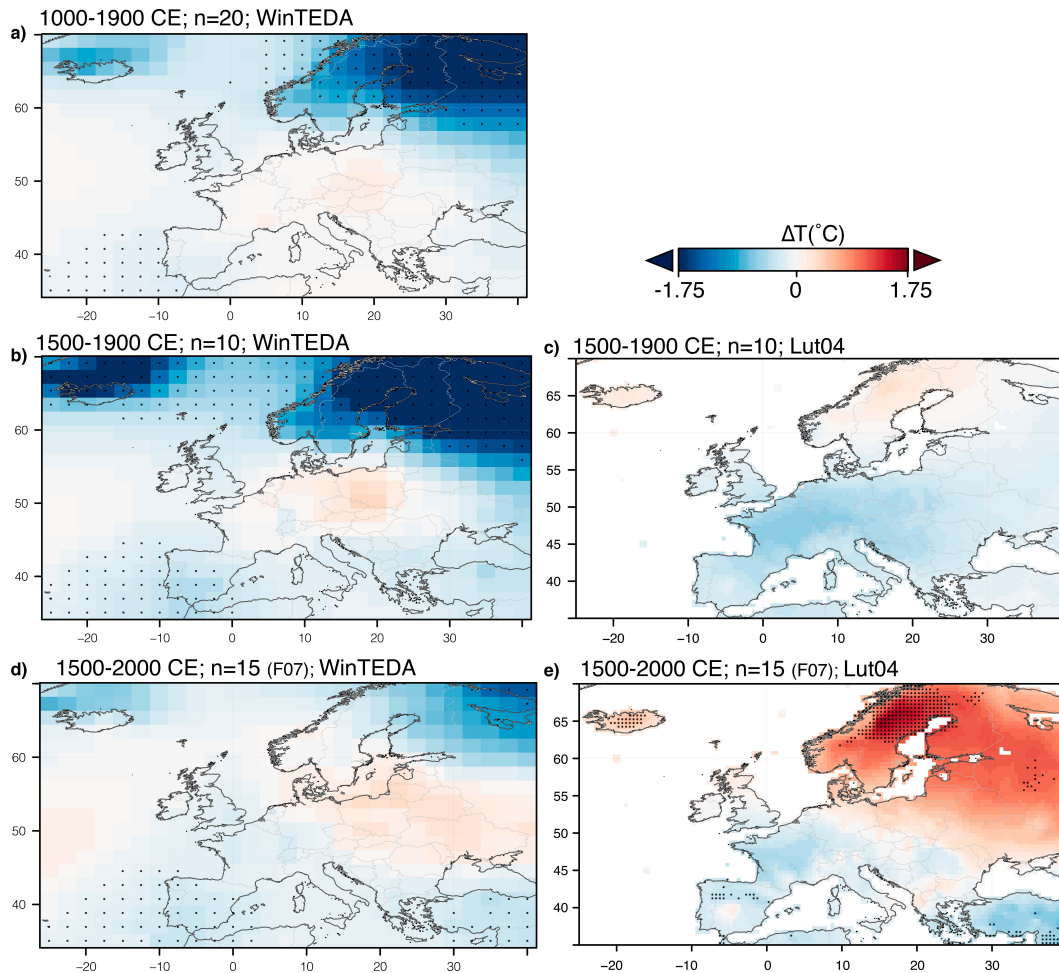


FIG. 8. SEA of European surface temperature anomalies in the first posteruption winter (DJF), over the area analyzed by F07. (a) The average of 20 eruptions larger than Pinatubo from 1500 to 2000 CE (TVE_{ev}; Table 1), using WinTEDA. Stippling indicates significant values at the 95% confidence level. (b) As in (a), but for the 10 eruptions between 1500 and 1900. (c) As in (b), but for using the LUT04 reconstruction. (d) As in (b), but for the 15 eruptions in F07. (e) As in (d), but for using the LUT04 dataset.

aerosols—was found to be larger in the *second* posteruption winters (see their Fig. 2), which is at odds with a stratospheric polar vortex impacting the NAO. Because we are aware of no physically plausible reason for expecting a circulation-driven temperature response in the second posteruption winter, our attempts to reconcile our results with those of F07 will now focus exclusively on the first posteruption winters.

We start by examining the average posteruption WinTEDA temperature anomalies for our 20 TVE_{ev} events, over the same Eurasian region used by F07. This SEA average, shown in Fig. 8a, reveals a statistically significant winter cooling in northern Europe, especially over Scandinavia and western Russia, as one might expect from the individual events shown in Fig. 2. This directly contradicts the winter warming shown in Fig. 2a of F07.

We bridge the gap between the F07 results and those in Fig. 8a in three steps. First, we limit our SEA to cover the same time period as F07, i.e., the last half millennium. Averaging solely

over the 10 TVE_{ev} events in the period 1500–1900 (those marked with an asterisk in Table 1), yields a strong Eurasian cooling in WinTEDA, shown in Fig. 8b. Second, using the same set of 10 events (all larger than Pinatubo), we repeat the SEA but with the LUT04 reconstruction used in F07. We find no posteruption warming in LUT04 from those 10 events (see Fig. 2c), all larger than Pinatubo. Third, using the same LUT04 reconstruction, we swap the 10 TVE_{ev} eruptions with the 15 eruptions in F07 (listed in Table A1). This yields a strong winter warming over northern Europe (seen in Fig. 8e), just as reported in Fig. 2a, F07.

Having independently reproduced the winter warming result in F07, we can now explain its origin. Before doing so, we close the loop by taking the same 15 events in F07 and performing an SEA using WinTEDA. The resulting average, plotted in Fig. 8d, shows no significant winter warming over central Europe and a much-reduced cooling over northern Europe. Obviously, the conclusion one reaches is *very* sensitive to the events included in the SEA and the reconstruction

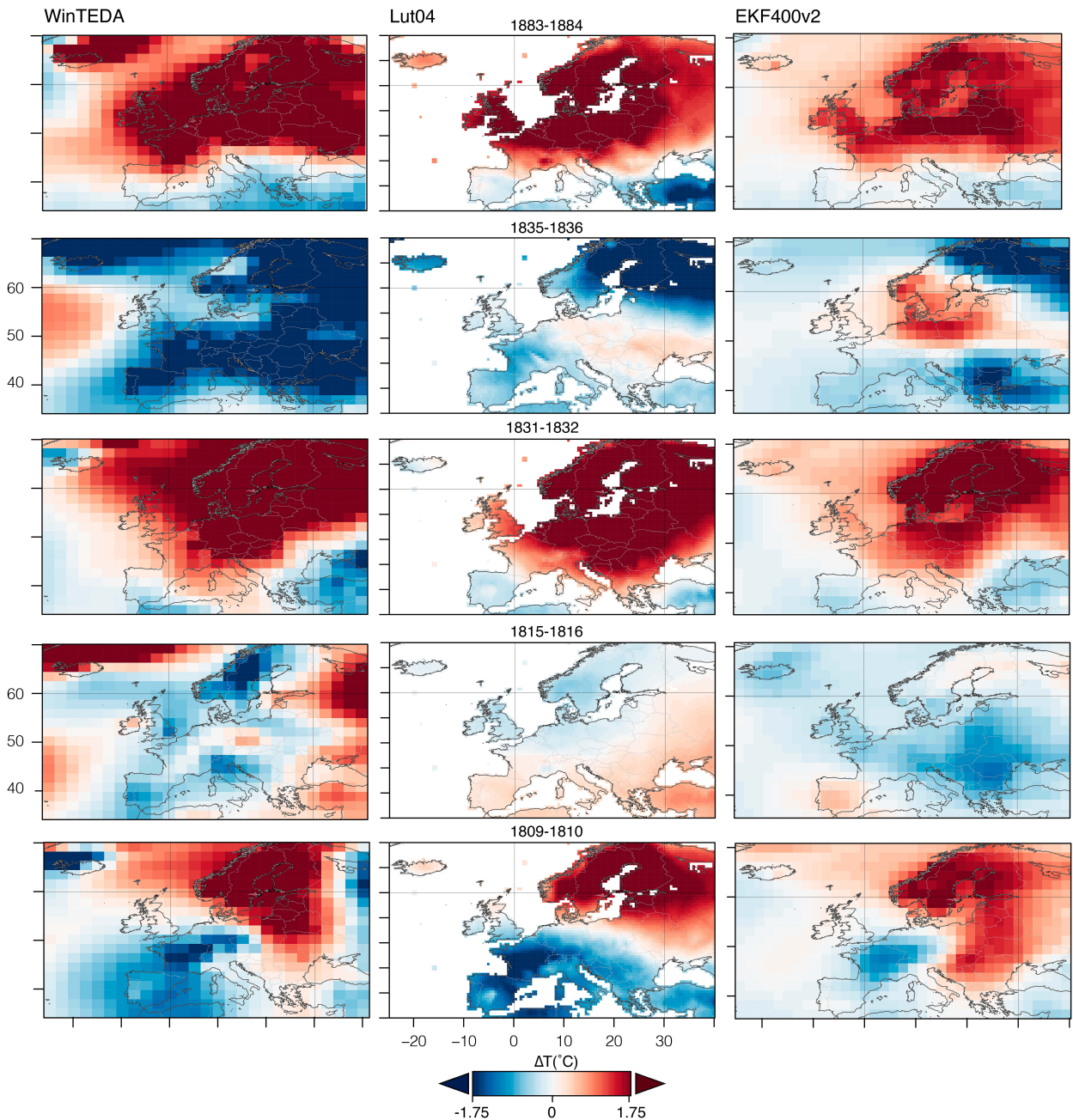


FIG. 9. First posteruption winter temperature anomalies for the nineteenth century TVE_{cv} events (see Table 1). (left) WinTEDA, (middle) LUT04, and (right) EKF400_v2.

used. Such sensitivity is typical of a *very weak forced signal*—an important conclusion, which confirms what many of the early studies repeatedly reported.

Next, we address three questions. First, contrasting in Figs. 8b and 8c, we ask: how do we explain the absence of strong cooling over northern Europe as we go from WinTEDA to LUT04? Second, contrasting in Figs. 8c and 8e, we ask: what causes the strong warming as we go from the 10 large events in TVE_{cv} to the 15 events in F07? Third, contrasting in Figs. 8b and 8d, we ask: why is the posteruption

cooling over Northern Europe greatly reduced when smaller eruptions are included in WinTEDA? We answer each in turn by comparing the temperature anomalies in WinTEDA and LUT04 for individual events.

First, to explain the differences between Figs. 8b and 8c, we divide the 10 larger-than-Pinatubo events over 1500–1900 (starred in Table 1) into two groups: five eruptions in the nineteenth century and the remaining five in the sixteenth and seventeenth centuries. For the former, shown in Fig. 9, with WinTEDA in the left column and LUT04 in the middle

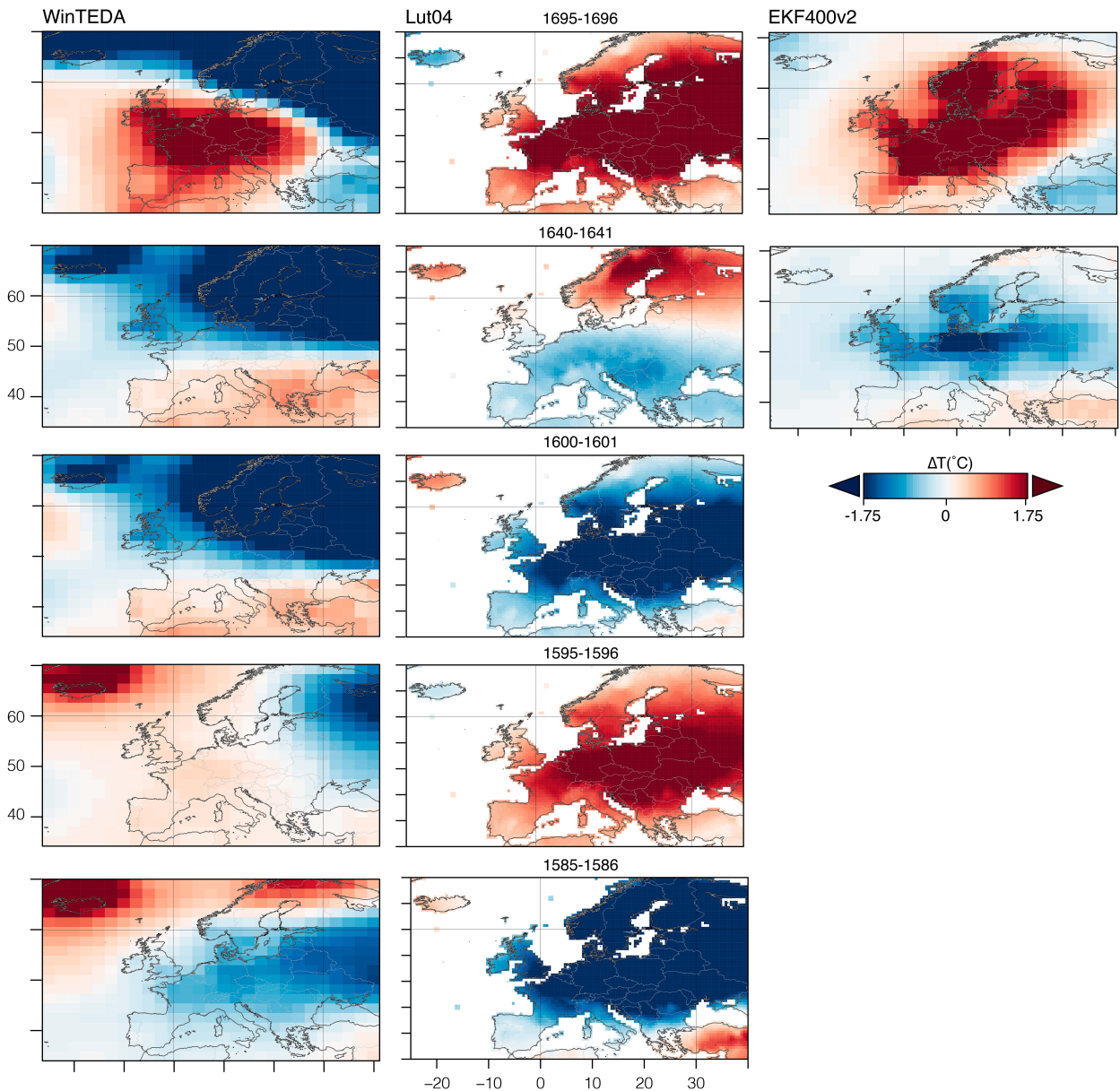


FIG. 10. As in Fig. 9, but for the seventeenth and sixteenth century TVE_{ev} events (see Table 1).

column, the anomalies are in overall agreement, except for 1815/16⁷ over southern Europe. For the latter, shown in Fig. 10, multiple considerable discrepancies can be seen,

⁷ Notably, we find a different response for the Iberian Peninsula and Italy, with warming in LUT04 and cooling WinTEDA. Since the LUT04 reconstruction, many efforts have been made to retrieve additional early instrumental data from European cities. Such is the case of the city of Barcelona (Prohom et al. 2012) which now has a long instrumental temperature series starting in 1780 (included in WinTEDA). By looking at the Tambora winter with respect to the five previous years' mean, we detect a cooling response (-0.64°C), which is in line with our study. We also find a cooling response of -1.78°C for the city of Milano (Maugeri et al. 2002).

notably the winters 1695/96, 1640/41, and 1595/96, where LUT04 anomalies (middle column) show large warming, while WinTEDA anomalies (left column) show cooling. Without entering into the detailed merits⁸ of each reconstruction, these large differences explain the muted cooling over northern Europe in Fig. 8c compared to Fig. 8b. The key point, however, is that if F07 had restricted their analysis to the 10 eruptions larger than Pinatubo, they would have reported a posteruption boreal winter cooling, not a warming.

⁸ We simply note here that several recent advances, not known at the time F07 was published, have now resulted in accurate dating of several events, notably 1586 (now 1585 with no uncertainty) and 1641 (now December 1640).

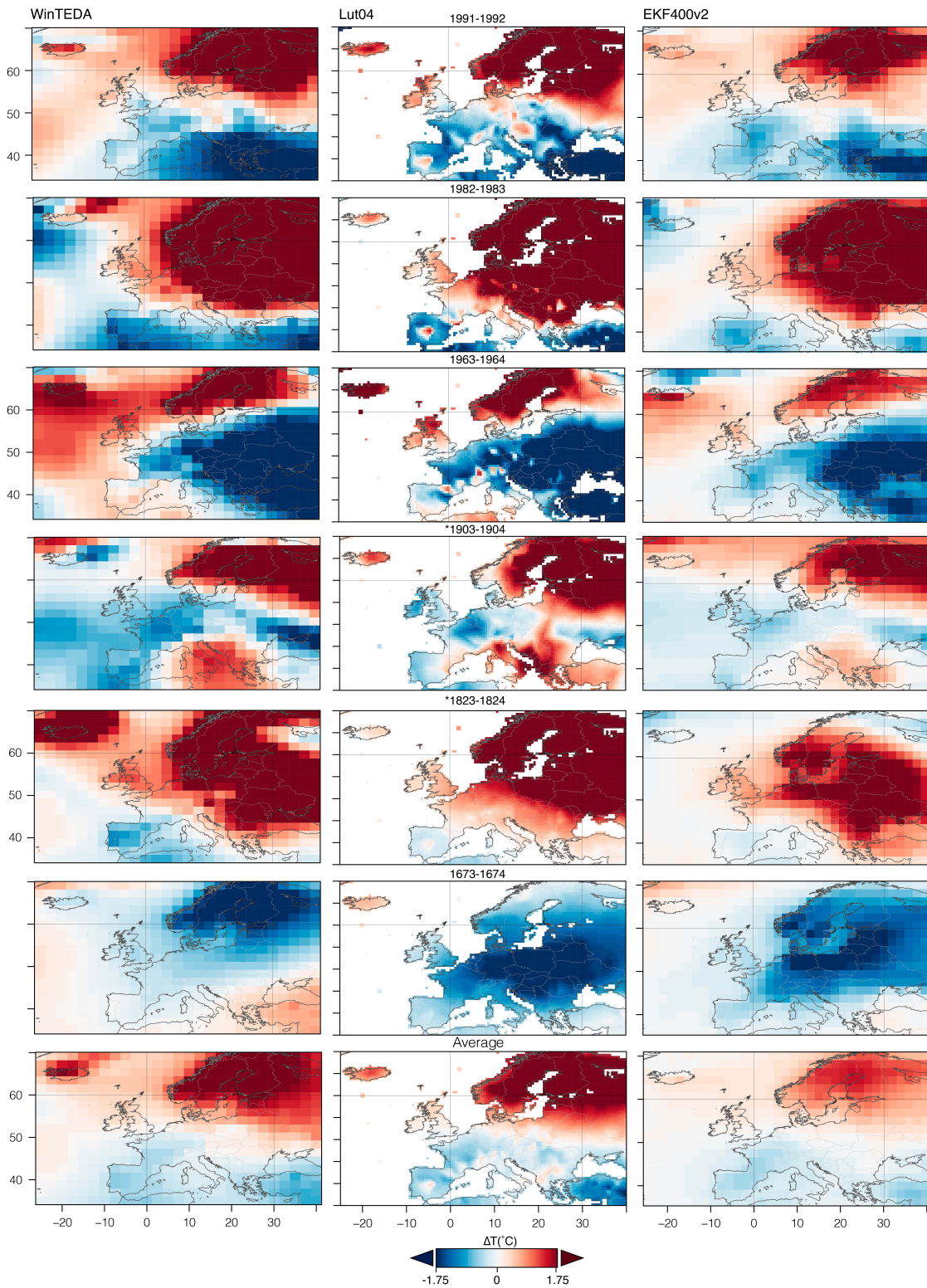


FIG. 11. As in Fig. 9, but for Pinatubo 1991 and five other smaller eruptions included in the F07 averaging, but not present in TVE_{ev}. Years with an * indicate that F07 subjectively selected the second winter after the eruption instead of the first.

This leads us to the second question: what causes the strong warming in Fig. 8e that is not seen in Fig. 8c? The answer lies in the small eruptions included in the SEA analysis in F07; these eruptions are illustrated in Fig. 11. Notice that, except for the winter of 1673, all of these events show considerable warming, in both reconstructions (in spite of some dating readjustment). The crucial point is this: if indeed volcanic aerosols cause winter warming, why would there be *more* warming when *weaker* eruptions are added to the SEA? If the SEA averaging is indeed capturing a forced response, Fig. 8d should show more warming than Fig. 8e because it includes larger eruptions. Because the opposite happens, we conclude that the SEA is actually adding a lot of noise and a very little signal, resulting in a larger warming that is *not* the forced response.

This is confirmed by addressing the third question. If, as Fig. 2 suggests, large eruptions are mostly followed by winter cooling over Eurasia, we would expect a *smaller* cooling when the *smaller* eruptions are included in the SEA averaging. This is indeed the case, as one can see comparing Fig. 8b with Fig. 8d, which both use the same WinTEDA reconstruction and only differ in the eruptions used.

c. Reichen et al. (2022)

The key point of the above discussion is that the original claim of F07—of a posteruption winter warming—simply cannot be reproduced with the WinTEDA dataset (as seen by comparing the two bottom panels in Fig. 8). At this point, then, the reader may wonder which dataset to believe. Fortunately, a third winter reconstruction is available: it is referred to as EKF400_v2 (Valler et al. 2022; Reichen et al. 2022), and we analyze it next. Since that dataset only extends back to 1600, only two of the five eruptions in Fig. 10 are available. Nonetheless, temperature anomalies for a total of seven eruptions in TVE_{ev} can be computed (Figs. 9 and 10), plus an additional six smaller eruptions included not in TVE_{ev} but in F07 (Fig. 11). We draw the reader's attention to several interesting points.

First, a visual comparison over Europe of EKF400_v2 and WinTEDA—contrast the right and left columns of Figs. 9–11—reveals an excellent agreement between the posteruption Eurasian winter anomalies in the two datasets. The only exception appears to be the Cosigüina eruption of 1835 (Fig. 9, second row), with cold anomalies in WinTEDA but warm anomalies in EKF400_v2. The temperature anomalies are otherwise very similar, providing mutual support to the robustness of both datasets.

Second, we notice a few large differences between the LUT04 dataset (which formed the basis of the F07 analysis) and EKF400_v2. In particular, the clear warming in northern Europe following the Parker eruption in 1640 is absent in EKF400_v2 (and in WinTEDA). Also, the 1815 Tambora eruption is followed by anomalous winter cooling in EKF400_v2 (and WinTEDA), but that cooling is largely absent in LUT04. These discrepancies likely contributed to the warming signal reported in F07, which is absent in the later reconstructions.

Third, enlarging the comparison to the entire Eurasian continent, let us consider the green boxplots in Fig. 3 that show the EKF400_v2 anomalies and compare them to the black

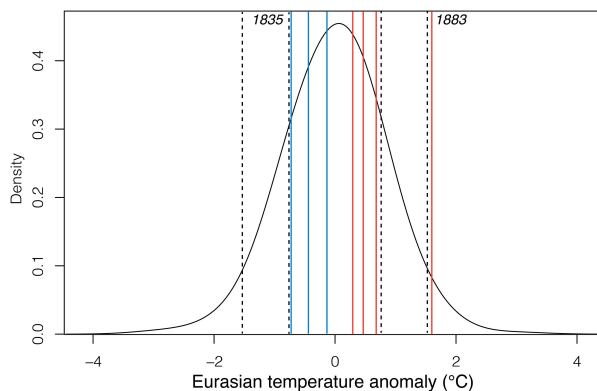


FIG. 12. As in Fig. 5, but for the EKF400_v2 reconstruction (Valler et al. 2022).

boxplots that show WinTEDA. Of the seven events common to WinTEDA and EKF400_v2, four have the same-signed anomalies in the two reconstructions (1640, 1883, 1831, and 1835). For the three remaining events (1695, 1809, and 1815), we limit ourselves to highlighting the large uncertainties across the members of each reconstruction. We summarize the EKF400_v2 results in Fig. 12: four posteruption winters have shown warm anomalies and three posteruption winters have shown cool anomalies. For the same eruptions in WinTEDA, three posteruption winters have shown warm anomalies and four posteruption winters have shown cool anomalies. Taking these results together, we conclude that there is no evidence for a posteruption winter warming from these large, low-latitude eruptions.

That same conclusion, as it happens, can also be reached from scrutinizing the supplemental material of a recent paper (Reichen et al. 2022), which made use of the same EKF400_v2 reconstruction discussed herein. In their Fig. S6, one finds the extended cold season (October–March) Eurasian posteruption surface temperature anomalies for the low-latitude volcanic eruptions in Sigl et al. (2015) over the period 1701–1905. Unsurprisingly, *averaging* over such eruptions, one finds *cold* anomalies over Eurasia, just as one would obtain by averaging the panels in Fig. 3 (which we deliberately avoid doing, as explained above).

5. Summary and discussion

We have built a new temperature reconstruction (WinTEDA) over the last millennium, specifically designed to determine whether anomalous surface warming over Eurasia can be seen in boreal winters following low-latitude eruptions with large stratospheric sulfur injections. We have examined 20 eruptions larger than the 1991 Pinatubo event in WinTEDA (which incorporates temperature observations and only proxies with signals maximized in the winter months), and we have found no evidence of a forced warming signal over Eurasia in the first⁹ winter

⁹ The curious reader will find the second posteruption winter anomalies in Fig. A1 and note the unsurprising absence of a warming signal in that winter as well.

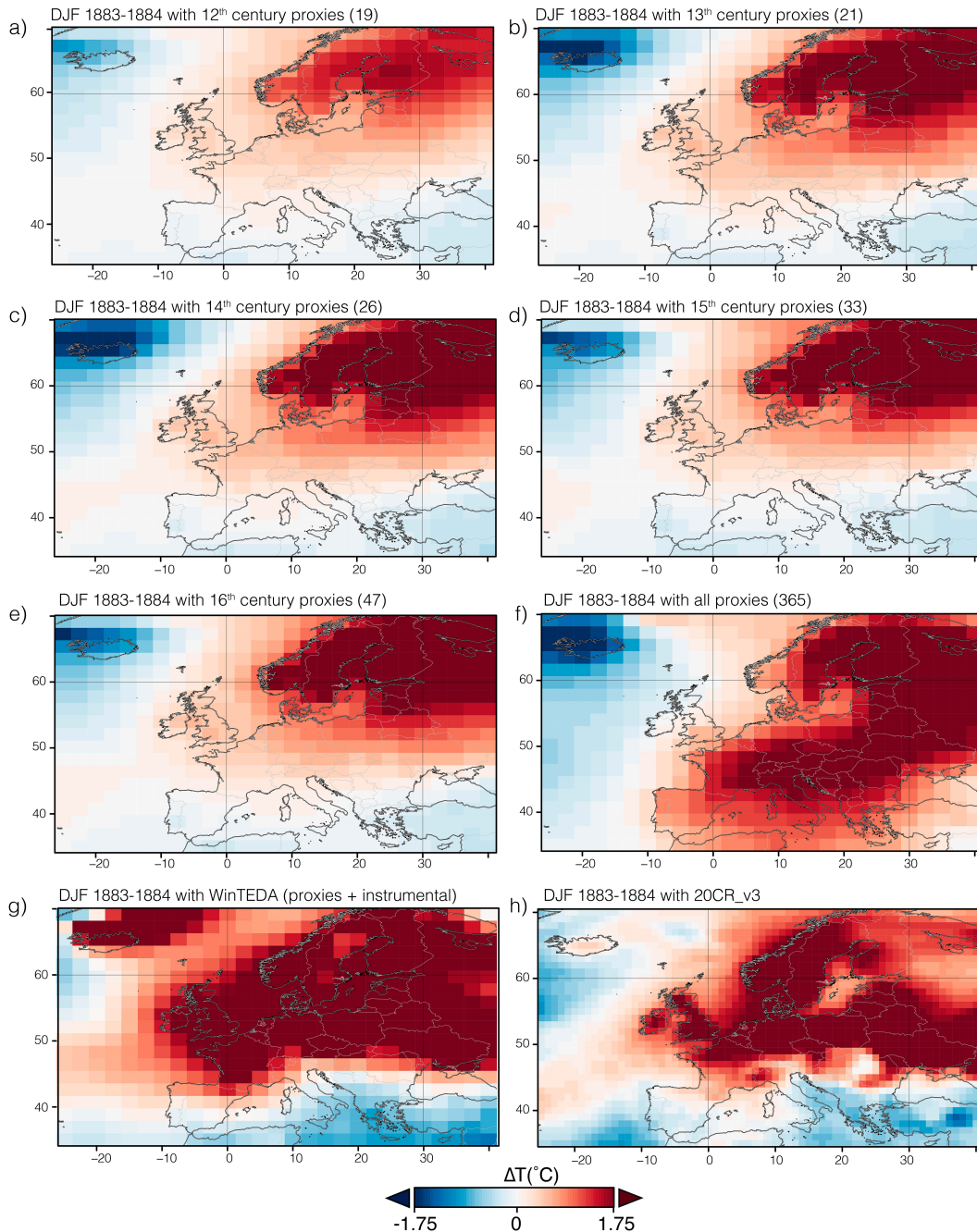


FIG. 13. Temperature anomalies in the first winter following the 1883 Krakatau eruption from modified versions of the WinTEDA reconstruction. (a)–(e) No instrumental data are used in the reconstructions, and only proxies dating back to the twelfth to the sixteenth century, respectively, are included (the number of proxies is given in parentheses). (f) Anomalies are computed from reconstructions with all available proxies *only*. (g) Anomalies in the full WinTEDA product, i.e., all proxies and instrumental data. (h) As a reference, we show the 20CR reanalysis (Compo et al. 2011) for the same winter.

following each event. This is the first important conclusion of our study.

Our conclusion differs from much of the previous literature because we have deliberately refrained from averaging together low- and high-latitude eruptions, first and second

posteruption winters, and, most importantly, large and small eruptions. None of these procedures can be firmly justified, and we have explicitly shown how earlier reports of a posteruption Eurasian winter warming were a consequence of combining incongruent events in the SEA average. Hence, the

second important conclusion of our study is that the widely used SEA method can be misleading when trying to identify the response to volcanic eruptions over small geographic regions, where the signal-to-noise ratio is likely to be small. We therefore suggest that future studies on the impact of volcanic eruptions on surface climate examine individual events and carefully test the robustness of any SEA averaging that includes both large and small eruptions.

The third important conclusion of our study is that—even for large eruptions, such as those we have considered herein—the volcanic signal needs to be examined and evaluated in the context of internal variability. Our analysis has shown that, in the winter months, the posteruption temperature anomalies over Eurasia for the 20 largest eruptions in the LM are, in most cases, less than 2σ of the internal variability. If confirmed by future studies, this implies that posteruption winters are unremarkable and thus difficult to distinguish from other winters over Eurasia. This is not the case for the posteruption summers, for which 12 of the 20 events fall outside the 2σ range and two events are outside the 4σ range.

While the lack of posteruption winter warming over Eurasia in three independently derived reconstructions leads us to conclude that large, low-latitude eruptions do not *in fact* cause Eurasian winter warming, one could object¹⁰ that such a conclusion is invalid and merely betrays “impatience with ambiguity” on the grounds that “the absence of evidence is not evidence of absence,” as famously noted by Sagan (1997). Or, more simply, since most trees do not grow in winter, it is possible that present-day reconstructions are simply incapable of capturing any winter warming although it may actually exist. To refute this objection, we offer the 1883 Krakatau eruption as evidence to the contrary.

Recall that the winter of 1883/84 was anomalously warm over Eurasia (Polvani and Camargo 2020), while the preceding summer was anomalously cold. Still focusing on the same domain as in Figs. 8–11, which is common to all the datasets we have analyzed here, in Fig. 13, we show the post-Krakatau winter temperature anomalies in a series of modified WinTEDA reconstructions with a progressively increasing number of proxies, from the oldest to the most recent century. In Fig. 13a, the reconstruction is based on assimilated proxies dating back to the twelfth century, while excluding instrumental data. In Fig. 13b, we did the same but with the thirteenth century proxies only; in Fig. 13c, we did the same with the fourteenth century proxies only; and so on until Fig. 13f, where all the proxies are included. In all these figure panels, a clear warming pattern emerges although no instrumental data are used. The warming becomes stronger once the instrumental data are added (Fig. 13g), and WinTEDA agrees with reanalysis (Fig. 13h). But the key point of Fig. 13 is that no instrumental data are needed to capture the warming that did occur in the first boreal winter after the 1883 Krakatau eruption. The absence of evidence *does* amount to evidence of absence here: we find no warming in the reconstruction because the eruptions did not cause any observable warming. While it is not unconceivable that uncertainties in the current datasets and dating of the eruptions may mask a tiny warming signal,

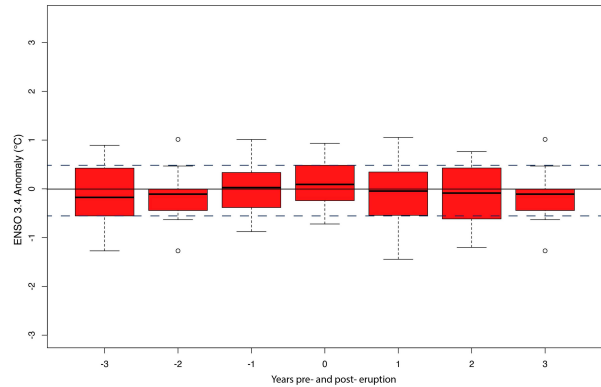


FIG. 14. The Niño-3.4 index, across the 20 TVE_{cv} events, from 3 years before to 3 years after the volcanic event (year 0) in the DJF season of the PHYDA ensemble mean (Steiger et al. 2018). The dark center line in each boxplot is the median, the edges of the boxes are 25th and 75th percentiles, and the whiskers extend to 1.5 standard deviations above or below the median. Thin horizontal dashed lines indicate the thresholds above or below which El Niño (positive) or La Niña (negative) events occur, respectively.

at this time, no dataset shows a consistent posteruption warming, hence our conclusion.

Some readers may wonder how we can reconcile the absence of Eurasian posteruption winter warming in reconstructions, with the findings of the two most recent modeling studies (Azoulay et al. 2021; DallaSanta and Polvani 2022) that have reported statistically significant posteruption winter Eurasian warming for large eruptions in their simulations. Avoiding any speculation as to why models may be unrealistically simulating the impact of volcanic eruptions on climate, the apparent inconsistency is easily resolved by appreciating two key findings of these studies. First, even for the largest eruptions of the last millennium, the forced warming in those models was found to be, at most, comparable to the internal variability. Second, statistical significance was obtained with large ensembles of simulations (as the signal-to-noise ratio can be made arbitrarily large by enlarging the ensemble). Hence, it is entirely plausible that with only twenty events, many of which were much smaller than the 1257 Samalas eruption, a small forced signal is simply overwhelmed by the noise in the reconstructions, leaving us with no evidence of a winter warming.

One might also wonder whether El Niño–Southern Oscillation (ENSO) may possibly impact the Eurasian winter temperature response to large eruptions. In a recent paper, Coupe and Robock (2021) have claimed that the presence of El Niño conditions over the tropical Pacific is crucial to produce postvolcanic winter warming, while two earlier studies reported that El Niño does not affect the posteruption Eurasian winter response (Christiansen 2008; Thomas et al. 2009b). Furthermore, El Niño conditions have been linked to a negative phase of the NAO (Li and Lau 2012), which would lead to Eurasian cooling, not warming. Regardless of these findings in the literature, given the present confusion as to whether ENSO affects the posteruption Eurasian winter temperatures, we have examined the Niño-3.4 index before and

¹⁰ We are grateful to one of the referees for proffering this objection.

after the 20 TVE_{ev} events larger than Pinatubo in the LM. We computed the index using the PHYDA ENSO reconstruction following the standard definition (Trenberth 1997). As one can see in Fig. 14s, the median Niño-3.4 index is neither consistently positive nor negative before, during, or after the 20 largest eruptions of the LM. This implies that ENSO is not a major player in the posteruption Eurasian winter temperature response. It also suggests that these very large eruptions do not cause an anomalous ENSO, confirming the findings of a number of previous studies (see, e.g., Dee et al. 2020; Dee and Steiger 2022; and Zhu et al. 2022, for the latest on this subject).

Finally, looking back at Figs. 2 and 3, one may be tempted to conclude that posteruption Eurasian winters are—on average— anomalously cold, as reported in Reichen et al. (2022). However, as already noted, we find no correlation between the stratospheric injection mass and the winter cooling anomalies, and this makes it difficult to suggest that the posteruption cooling is caused by the preceding eruption. For this reason, we have decided to limit our claim to a null result: *the absence of a robust posteruption Eurasian winter warming*. This null result, nonetheless, challenges the original claim of Robock and Mao (1992) and of much of the subsequent literature. It is therefore important that future studies—using new temperature reconstructions, improved dating techniques, and increased proxy networks— independently corroborate (or invalidate) our findings. For the time being, our results suggest a much simpler story than the complex stratospheric pathway mechanism: namely, that large, low-latitude eruptions cause a small surface cooling—not only globally but even in winter over Eurasia—as one would naively expect.

Acknowledgments. E. T. is funded by a Marie Skłodowska-Curie Action (ITHACA-101024389). N. J. S., J. E. S., and M. V. were partially supported by NSF-PIRE (OISE-1743738). M. V. was partially supported by NSF-CNH2 (DEB-1923957). This work was also funded, in part, by Awards 1914569 and 2303352 from the U.S. National Science Foundation to Columbia University. The authors also wish to express their gratitude to the three highly critical reviewers whose suggestions greatly improved the manuscript.

Data availability statement. The Winter Temperature Eurasian Data Assimilation Reconstruction (WinTEDA) can be downloaded from <https://doi.org/10.5281/zenodo.6806314>.

APPENDIX

Miscellanea

a. Eruptions analyzed by F07

For completeness, we append here the list of 15 eruptions analyzed in F07. The ones marked with an asterisk are those not included in our 20 TVE_{ev} set and shown in Fig. 11.

b. Second posteruption winter temperature anomalies

At the suggestion of two reviewers, we have computed the *second* posteruption winter anomalies in WinTEDA for the 20 large eruptions in TEV_{ev} (see Table 1). As can be seen in Fig. A1, of the 20 eruptions, 14 are anomalously cold and 6 are anomalously warm, when averaging over the Eurasian box, in the second winter. There is, again, no evidence of warming in this second posteruption winter.

TABLE A1. Tropical volcanic eruptions used by F07 and the dating they used. We have used TS17 for the dating of our TVE_{ev} events. The symbol “-/-” indicates that there is no difference in dating between F07 and TS17. The VSSI estimate and uncertainty (σ) are from TS17. Asterisks highlight the smaller eruptions included in the SEA averaging in F07 but not in our main analysis.

Name	CE year	DJF year	TS17 dating	VSSI	VSSI (σ)
*Pinatubo	1991	1992	-/-	8.78	2.23
*El Chichon	1982	1983	-/-	2.65	0.90
*Agung	1963	1964	-/-	5.22	
*Santa Maria	1902	1904	-/-	3.14	0.78
Krakatoa	1883	1884	-/-	9.34	1.91
Cosiguina	1835	1836	-/-	9.48	2.21
Babuyan Claro	1831	1831	-/-	12.98	3.41
*Galunggung	1822	1824	-/-	2.02	0.79
Tambora	1815	1816	-/-	28.08	4.49
Unknown	1809	1810	-/-	19.26	3.54
*Gamkonora	1673	1674	-/-	4.67	0.82
Parker	1641	1642	1640	18.68	4.28
Huaynaputina	1600	1601	-/-	18.95	4.03
Nevado del Ruiz	1595	1597	-/-	8.87	1.51
Kelut	1586	1587	1585	8.51	2.34

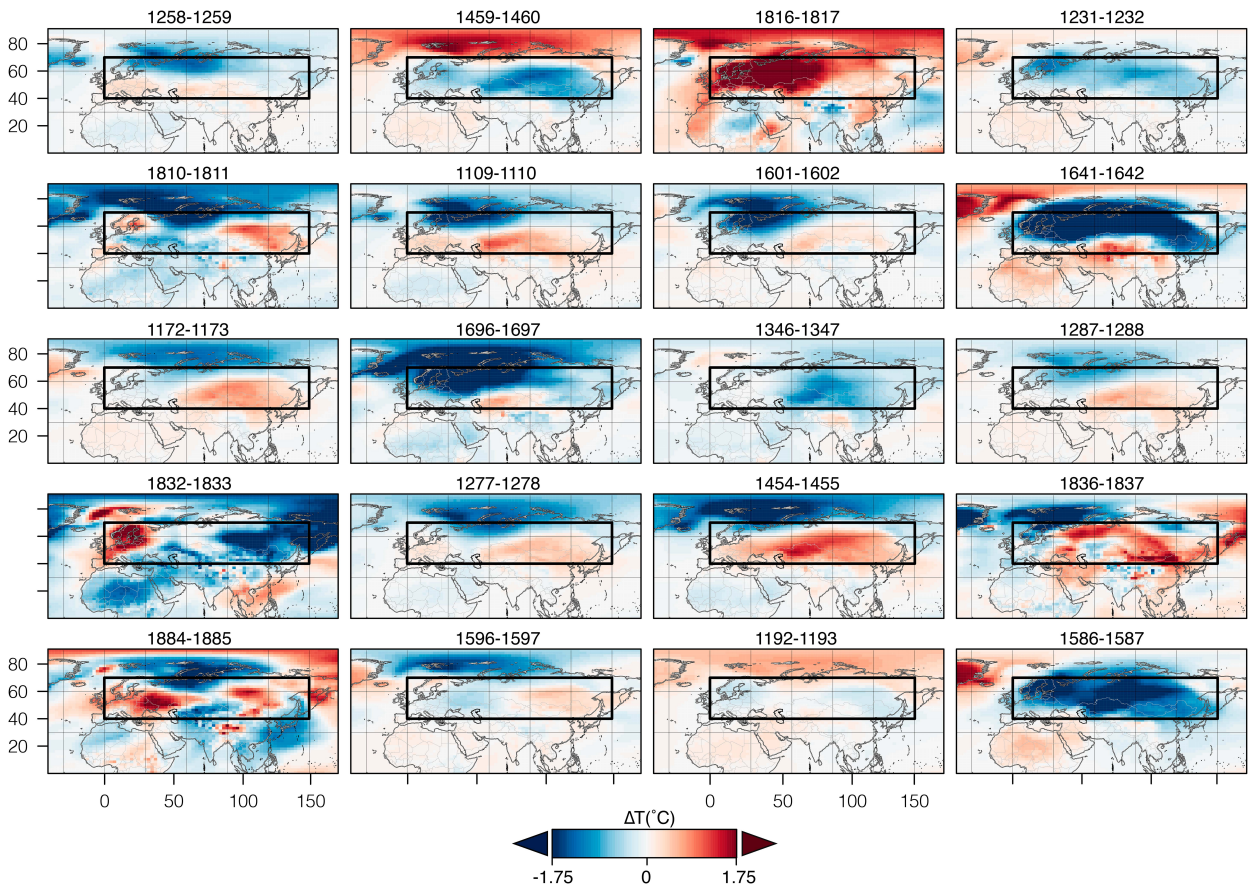


FIG. A1. As in Fig. 2, but for the second posteruption winter.

REFERENCES

- Anchukaitis, K. J., B. M. Buckley, E. R. Cook, B. I. Cook, R. D. D'Arrigo, and C. M. Ammann, 2010: Influence of volcanic eruptions on the climate of the Asian monsoon region. *Geophys. Res. Lett.*, **37**, L22703, <https://doi.org/10.1029/2010GL044843>.
- Azoulay, A., H. Schmidt, and C. Timmreck, 2021: The Arctic polar vortex response to volcanic forcing of different strengths. *J. Geophys. Res. Atmos.*, **126**, e2020JD034450, <https://doi.org/10.1029/2020JD034450>.
- Baldwin, M. P., and T. J. Dunkerton, 2001: Stratospheric harbingers of anomalous weather regimes. *Science*, **294**, 581–584, <https://doi.org/10.1126/science.1063315>.
- , D. B. Stephenson, D. W. J. Thompson, T. J. Dunkerton, A. J. Charlton, and A. O'Neill, 2003: Stratospheric memory and skill of extended-range weather forecasts. *Science*, **301**, 636–640, <https://doi.org/10.1126/science.1087143>.
- Bittner, M., 2015: On the discrepancy between observed and simulated dynamical responses of Northern Hemisphere winter climate to large tropical volcanic eruptions. Ph.D. thesis, University of Hamburg, 142 pp., https://pure.mpg.de/rest/items/item_2239264/component/file_2239290/content.
- , H. Schmidt, C. Timmreck, and F. Sienz, 2016: Using a large ensemble of simulations to assess the Northern Hemisphere stratospheric dynamical response to tropical volcanic eruptions and its uncertainty. *Geophys. Res. Lett.*, **43**, 9324–9332, <https://doi.org/10.1002/2016GL070587>.
- Christiansen, B., 2008: Volcanic eruptions, large-scale modes in the Northern Hemisphere, and the El Niño–Southern Oscillation. *J. Climate*, **21**, 910–922, <https://doi.org/10.1175/2007JCLI1657.1>.
- Compo, G. P., 2011: The Twentieth Century Reanalysis Project. *Quart. J. Roy. Meteor. Soc.*, **137** (654), 1–28, <https://doi.org/10.1002/qj.776>.
- Cook, E. R., Y. Kushnir, J. E. Smerdon, A. P. Williams, K. J. Anchukaitis, and E. R. Wahl, 2019: A Euro-Mediterranean tree-ring reconstruction of the winter NAO index since 910 C.E. *Climate Dyn.*, **53**, 1567–1580, <https://doi.org/10.1007/s00382-019-04696-2>.
- Coupe, J., and A. Robock, 2021: The influence of stratospheric soot and sulfate aerosols on the Northern Hemisphere wintertime atmospheric circulation. *J. Geophys. Res.*, **126**, e2020JD034513, <https://doi.org/10.1029/2020JD034513>.
- Crowley, T. J., and M. B. Unterman, 2013: Technical details concerning development of a 1200 yr proxy index for global volcanism. *Earth Syst. Sci. Data*, **5**, 187–197, <https://doi.org/10.5194/essd-5-187-2013>.
- DallaSanta, K., and L. M. Polvani, 2022: Volcanic stratospheric injections up to 160 Tg(S) yield a Eurasian winter warming indistinguishable from internal variability. *Atmos. Chem. Phys.*, **22**, 8843–8862, <https://doi.org/10.5194/acp-22-8843-2022>.
- Dee, S. G., and N. J. Steiger, 2022: ENSO's response to volcanism in a data-assimilation-based paleoclimate reconstruction over the

- Common Era. *Paleoceanogr. Paleoclimatol.*, **37**, e2021PA004290, <https://doi.org/10.1029/2021PA004290>.
- , K. M. Cobb, J. Emile-Geay, T. R. Ault, R. L. Edwards, H. Cheng, and C. D. Charles, 2020: No consistent ENSO response to volcanic forcing over the last millennium. *Science*, **367**, 1477–1481, <https://doi.org/10.1126/science.aax2000>.
- Driscoll, S., A. Bozzo, L. J. Gray, A. Robock, and G. Stenchikov, 2012: Coupled Model Intercomparison Project 5 (CMIP5) simulations of climate following volcanic eruptions. *J. Geophys. Res.*, **117**, D17105, <https://doi.org/10.1029/2012JD017607>.
- Fischer, E. M., J. Luterbacher, E. Zorita, S. F. B. Tett, C. Casty, and H. Wanner, 2007: European climate response to tropical volcanic eruptions over the last half millennium. *Geophys. Res. Lett.*, **34**, L05707, <https://doi.org/10.1029/2006GL027992>.
- Gao, C., A. Robock, and C. Ammann, 2008: Volcanic forcing of climate over the past 1500 years: An improved ice core-based index for climate models. *J. Geophys. Res.*, **113**, D23111, <https://doi.org/10.1029/2008JD010239>.
- Graft, H.-F., I. Kirchner, A. Robock, and I. Schult, 1993: Pinatubo eruption winter climate effects: Model versus observations. *Climate Dyn.*, **9**, 81–93, <https://doi.org/10.1007/BF00210011>.
- Groisman, P. Ya., 1992: Possible regional climate consequences of the Pinatubo eruption: An empirical approach. *Geophys. Res. Lett.*, **19**, 1603–1606, <https://doi.org/10.1029/92GL01474>.
- Haurwitz, M. W., and G. W. Brier, 1981: A critique of the superposed epoch analysis method: Its application to solar–weather relations. *Mon. Wea. Rev.*, **109**, 2074–2079, [https://doi.org/10.1175/1520-0493\(1981\)109<2074:ACOTSE>2.0.CO;2](https://doi.org/10.1175/1520-0493(1981)109<2074:ACOTSE>2.0.CO;2).
- Hegerl, G. C., T. J. Crowley, S. K. Baum, K.-Y. Kim, and W. T. Hyde, 2003: Detection of volcanic, solar and greenhouse gas signals in paleo-reconstructions of Northern Hemispheric temperature. *Geophys. Res. Lett.*, **30**, 1242, <https://doi.org/10.1029/2002GL016635>.
- Jones, P. D., A. Moberg, T. J. Osborn, and K. R. Briffa, 2003: Surface climate responses to explosive volcanic eruptions seen in long European temperature records and mid-to-high latitude tree-ring density around the Northern Hemisphere. *Volcanism and the Earth's Atmosphere. Geophys. Monogr.*, Vol. 139, Amer. Geophys. Union, 239–254, <https://doi.org/10.1029/139GM15>.
- Kelly, P. M., P. D. Jones, and J. Penqun, 1996: The spatial response of the climate system to explosive volcanic eruptions. *Int. J. Climatol.*, **16**, 537–550, [https://doi.org/10.1002/\(SICI\)1097-0088\(199605\)16:5<537::AID-JOC23>3.0.CO;2-F](https://doi.org/10.1002/(SICI)1097-0088(199605)16:5<537::AID-JOC23>3.0.CO;2-F).
- Kirchner, I., G. L. Stenchikov, H.-F. Graf, A. Robock, and J. C. Antuña, 1999: Climate model simulation of winter warming and summer cooling following the 1991 Mount Pinatubo volcanic eruption. *J. Geophys. Res.*, **104**, 19039–19055, <https://doi.org/10.1029/1999JD900213>.
- Kodera, K., 1994: Influence of volcanic eruptions on the troposphere through stratospheric dynamical processes in the Northern Hemisphere winter. *J. Geophys. Res.*, **99**, 1273–1282, <https://doi.org/10.1029/93JD02731>.
- Li, Y., and N.-C. Lau, 2012: Impact of ENSO on the atmospheric variability over the North Atlantic in late winter—Role of transient eddies. *J. Climate*, **25**, 320–342, <https://doi.org/10.1175/JCLI-D-11-00037.1>.
- Luterbacher, J., D. Dietrich, E. Xoplaki, M. Grosjean, and H. Wanner, 2004: European seasonal and annual temperature variability, trends, and extremes since 1500. *Science*, **303**, 1499–1503, <https://doi.org/10.1126/science.1093877>.
- Maher, N., and Coauthors, 2019: The Max Planck Institute Grand Ensemble: Enabling the exploration of climate system variability. *J. Adv. Model. Earth Syst.*, **11**, 2050–2069, <https://doi.org/10.1029/2019MS001639>.
- Maugeri, M., L. Buffoni, B. Delmonte, and A. Fassina, 2002: Daily Milan Temperature and Pressure Series (1763–1998): Completing and homogenising the data. *Climatic Change*, **53**, 119–149, <https://doi.org/10.1023/A:1014923027396>.
- Nash, J. E., and J. V. Sutcliffe, 1970: River flow forecasting through conceptual models Part I—A discussion of principles. *J. Hydrol.*, **10**, 282–290, [https://doi.org/10.1016/0022-1694\(70\)90255-6](https://doi.org/10.1016/0022-1694(70)90255-6).
- Ortega, P., F. Lehner, D. Swingedouw, V. Masson-Delmotte, C. C. Raible, M. Casado, and P. Yiou, 2015: A model-tested North Atlantic Oscillation reconstruction for the past millennium. *Nature*, **523**, 71–74, <https://doi.org/10.1038/nature14518>.
- Osman, M. B., S. Coats, S. B. Das, J. R. McConnell, and N. Chellman, 2021: North Atlantic jet stream projections in the context of the past 1,250 years. *Proc. Natl. Acad. Sci. USA*, **118**, e2104105118, <https://doi.org/10.1073/pnas.2104105118>.
- Otto-Bliesner, B. L., and Coauthors, 2016: Climate variability and change since 850 CE: An ensemble approach with the Community Earth System Model. *Bull. Amer. Meteor. Soc.*, **97**, 735–754, <https://doi.org/10.1175/BAMS-D-14-00233.1>.
- Polvani, L. M., and S. J. Camargo, 2020: Scant evidence for a volcanically forced winter warming over Eurasia following the Krakatau eruption of August 1883. *Atmos. Chem. Phys.*, **20**, 13 687–13 700, <https://doi.org/10.5194/acp-20-13687-2020>.
- , A. Banerjee, and A. Schmidt, 2019: Northern Hemisphere continental winter warming following the 1991 Mt. Pinatubo Eruption: Reconciling models and observations. *Atmos. Chem. Phys.*, **19**, 6351–6366, <https://doi.org/10.5194/acp-19-6351-2019>.
- Prohom, M., M. Barriendos, E. Aguilar, and R. Ripoll, 2012: Recuperación y análisis de la serie de temperatura diaria de Barcelona, 1780–2011. *Cambio Climático. Extremos e Impactos*, Vol. 8, Asociación Española de Climatología, 207–217.
- Rao, M. P., and Coauthors, 2017: European and Mediterranean hydroclimate responses to tropical volcanic forcing over the last millennium. *Geophys. Res. Lett.*, **44**, 5104–5112, <https://doi.org/10.1002/2017GL073057>.
- Reichen, L., and Coauthors, 2022: A decade of cold Eurasian winters reconstructed for the early 19th century. *Nat. Commun.*, **13**, 2116, <https://doi.org/10.1038/s41467-022-29677-8>.
- Robock, A., and J. Mao, 1992: Winter warming from large volcanic eruptions. *Geophys. Res. Lett.*, **19**, 2405–2408, <https://doi.org/10.1029/92GL02627>.
- , and —, 1995: The volcanic signal in surface temperature observations. *J. Climate*, **8**, 1086–1103, [https://doi.org/10.1175/1520-0442\(1995\)008<1086:TVSIST>2.0.CO;2](https://doi.org/10.1175/1520-0442(1995)008<1086:TVSIST>2.0.CO;2).
- Rohde, R. A., and Z. Hausfather, 2020: The Berkeley Earth land/ocean temperature record. *Earth Syst. Sci. Data*, **12**, 3469–3479, <https://doi.org/10.5194/essd-12-3469-2020>.
- Sagan, C., 1997: *The Demon-Haunted World: Science as a Candle in the Dark*. Random House Publishing Group, 457 pp.
- Shindell, D. T., G. A. Schmidt, M. E. Mann, and G. Faluvegi, 2004: Dynamic winter climate response to large tropical volcanic eruptions since 1600. *J. Geophys. Res.*, **109**, D05104, <https://doi.org/10.1029/2003JD004151>.
- Sigl, M., and Coauthors, 2015: Timing and climate forcing of volcanic eruptions for the past 2,500 years. *Nature*, **523**, 543–549, <https://doi.org/10.1038/nature14565>.
- Steiger, N. J., J. E. Smerdon, E. R. Cook, and B. I. Cook, 2018: A reconstruction of global hydroclimate and dynamical variables over the Common Era. *Sci. Data*, **5**, 180086, <https://doi.org/10.1038/sdata.2018.86>.

- Stenchikov, G., K. Hamilton, R. J. Stouffer, A. Robock, V. Ramaswamy, B. Santer, and H.-F. Graf, 2006: Arctic oscillation response to volcanic eruptions in the IPCC AR4 climate models. *J. Geophys. Res.*, **111**, D07107, <https://doi.org/10.1029/2005JD006286>.
- Stoffel, M., and Coauthors, 2015: Estimates of volcanic-induced cooling in the Northern Hemisphere over the past 1,500 years. *Nat. Geosci.*, **8**, 784–788, <https://doi.org/10.1038/ngeo2526>.
- Tardif, R., and Coauthors, 2019: Last millennium reanalysis with an expanded proxy database and seasonal proxy modeling. *Climate Past*, **15**, 1251–1273, <https://doi.org/10.5194/cp-15-1251-2019>.
- Tejedor, E., N. J. Steiger, J. E. Smerdon, R. Serrano-Notivoli, and M. Vuille, 2021a: Global hydroclimatic response to tropical volcanic eruptions over the last millennium. *Proc. Natl. Acad. Sci. USA*, **118**, e2019145118, <https://doi.org/10.1073/pnas.2019145118>.
- , N. Steiger, J. E. Smerdon, R. Serrano-Notivoli, and M. Vuille, 2021b: Global temperature responses to large tropical volcanic eruptions in paleo data assimilation products and climate model simulations over the last millennium. *Paleoceanogr. Paleoclimatol.*, **36**, e2020PA004128, <https://doi.org/10.1029/2020PA004128>.
- Thomas, M. A., M. A. Giorgetta, C. Timmreck, H.-F. Graf, and G. Stenchikov, 2009a: Simulation of the climate impact of Mt. Pinatubo eruption using ECHAM5 – Part II: Sensitivity to the phase of the QBO and ENSO. *Atmos. Chem. Phys.*, **9**, 3001–3009, <https://doi.org/10.5194/acp-9-3001-2009>.
- , C. Timmreck, M. A. Giorgetta, H.-F. Graf, and G. Stenchikov, 2009b: Simulation of the climate impact of Mt. Pinatubo eruption using ECHAM5 – Part I: Sensitivity to the modes of atmospheric circulation and boundary conditions. *Atmos. Chem. Phys.*, **9**, 757–769, <https://doi.org/10.5194/acp-9-757-2009>.
- Toohey, M., and M. Sigl, 2017: Volcanic stratospheric sulfur injections and aerosol optical depth from 500 BCE to 1900 CE. *Earth Syst. Sci. Data*, **9**, 809–831, <https://doi.org/10.5194/essd-9-809-2017>.
- , and —, 2019: Reconstructed volcanic stratospheric sulfur injections and aerosol optical depth, 500 BCE to 1900 CE, version 3. World Data Center for Climate (WDCC), https://doi.org/10.26050/WDCC/eVolv2k_v3.
- , K. Krüger, M. Bittner, C. Timmreck, and H. Schmidt, 2014: The impact of volcanic aerosol on the Northern Hemisphere stratospheric polar vortex: Mechanisms and sensitivity to forcing structure. *Atmos. Chem. Phys.*, **14**, 13 063–13 079, <https://doi.org/10.5194/acp-14-13063-2014>.
- , B. Stevens, H. Schmidt, and C. Timmreck, 2016: Easy Volcanic Aerosol (EVA v1. 0): An idealized forcing generator for climate simulations. *Geosci. Model Dev.*, **9**, 4049–4070, <https://doi.org/10.5194/gmd-9-4049-2016>.
- Trenberth, K. E., 1997: The definition of El Niño. *Bull. Amer. Meteor. Soc.*, **78**, 2771–2777, [https://doi.org/10.1175/1520-0477\(1997\)078<2771:TDOENO>2.0.CO;2](https://doi.org/10.1175/1520-0477(1997)078<2771:TDOENO>2.0.CO;2).
- Valler, V., J. Franke, Y. Brugnara, and S. Brönnimann, 2022: An updated global atmospheric paleo-reanalysis covering the last 400 years. *Geosci. Data J.*, **9**, 89–107, <https://doi.org/10.1002/gdj3.121>.
- Wunderlich, F., and D. M. Mitchell, 2017: Revisiting the observed surface climate response to large volcanic eruptions. *Atmos. Chem. Phys.*, **17**, 485–499, <https://doi.org/10.5194/acp-17-485-2017>.
- Zambri, B., and A. Robock, 2016: Winter warming and summer monsoon reduction after volcanic eruptions in Coupled Model Intercomparison Project 5 (CMIP5) simulations. *Geophys. Res. Lett.*, **43**, 10 920–10 928, <https://doi.org/10.1002/2016GL070460>.
- Zhu, F., J. Emile-Geay, K. J. Anchukaitis, G. J. Hakim, A. T. Wittenberg, M. S. Morales, M. Toohey, and J. King, 2022: A re-appraisal of the ENSO response to volcanism with paleo-climate data assimilation. *Nat. Commun.*, **13**, 747, <https://doi.org/10.1038/s41467-022-28210-1>.